

1 **Quantifying groundwater dependence of a sub-polar lake**
2 **cluster in Finland using an isotope mass balance approach**

3

4 **Elina Isokangas¹, Kazimierz Rozanski², Pekka M. Rossi¹, Anna-Kaisa Ronkanen¹,**
5 **Bjørn Kløve¹**

6 [1] {Water Resources and Environmental Engineering Research Group, University of Oulu, P.O.
7 Box 4300, 90014 Oulun yliopisto, Finland}

8 [2] {Faculty of Physics and Applied Computer Science, AGH University of Science and
9 Technology, 30 Mickiewicza Av., 30-059 Krakow, Poland}

10 Corresponding author: Elina Isokangas, Email: elina.isokangas@oulu.fi Tel: +358414365252

11

12

13 **Abstract**

14 A stable isotope study of 67 kettle lakes and ponds situated on an esker aquifer (90 km²) in northern
15 Finland was carried out to determine the role and extent of groundwater inflow in groundwater-
16 dependent lakes. Distinct seasonal fluctuations in the $\delta^{18}\text{O}$ and $\delta^2\text{H}$ values of lakes are the result of
17 seasonal ice cover prohibiting evaporation during the winter. An iterative isotope mass balance
18 approach was used to calculate the inflow-to-evaporation ratios (I_{TOT}/E) of all 67 lakes during the
19 summer of 2013 when the isotopic compositions of the lakes were approaching a steady-state. The
20 balance calculations were carried out independently for ²H and ¹⁸O data. Since evaporation rates were
21 derived independently of any mass balance considerations, it was possible to determine the total
22 inflow (I_{TOT}) and mean turnover time (MTT) of the lakes. Furthermore, the groundwater seepage rates
23 to all studied lakes were calculated. A quantitative measure was introduced for the dependence of a
24 lake on groundwater (G index) that is defined as the percentage contribution of groundwater inflow
25 to the total inflow of water to the given lake. The G index values of the lakes studied ranged from ca.
26 39 % to 98 %, revealing generally large groundwater dependency among the studied lakes. This study
27 shows the effectiveness of applying an isotope mass balance approach to quantify the groundwater
28 reliance of lakes situated in a relatively small area with similar climatic conditions.

29

30 **Key words**

31 Stable isotopes of water, groundwater-surface water interaction, lake hydrology, mean turnover time
32 (MTT), inflow-to-evaporation ratio (I_{TOT}/E), thermal imaging

33 1. Introduction

34 The characterisation of groundwater dependent ecosystems (GDEs) is a requirement of the
35 Groundwater Directive (EC, 2006). These systems are often complex and their hydrology and contact
36 with aquifers are not well established. Lakes can be dependent on groundwater directly or indirectly,
37 and this dependence can vary over time (Kløve et al., 2011). Understanding groundwater and lake
38 water interaction is important not only for water resource management (Showstack, 2004), but also
39 for understanding the ecology and eutrophication of lakes, since groundwater may be a key element
40 in the lake nutrient balance (Ala-aho et al., 2013; Belanger et al., 1985; Brock et al., 1982; Kidmose
41 et al., 2013). Furthermore, the vulnerability of lakes to pollution can be controlled by their
42 dependency on groundwater (Kløve et al., 2011). Methods such as seepage meters (Ala-aho et al.,
43 2013; Rosenberry et al., 2008, 2013), environmental tracers (e.g. Dinçer, 1968; Shaw et al., 2013;
44 Stets et al., 2010; Yehdegho et al., 1997; Zuber, 1983) and numerical modelling (e.g. Krabbenhoft et
45 al., 1990; Stichler et al., 2008; Winter and Carr, 1980) can be used to determine the groundwater
46 reliance of lakes.

47 Heavy stable isotopes of water (^{18}O , ^2H) can be considered as ideal tracers for studying the
48 hydrological cycle (e.g. Clark and Fritz, 1997). Fractionation of isotopes of water is the very factor
49 enabling their use in hydrological studies, as it governs the changes in isotopic abundances within the
50 water cycle (Gat, 2010). At a global scale, the ^2H and ^{18}O isotope composition of meteoric waters
51 cluster along the line called the global meteoric water line (GMWL), first determined by Craig (1961):
52 $\delta^2\text{H} = 8 \cdot \delta^{18}\text{O} + 10$. Locally, this linear relationship may have a slightly different form (local
53 meteoric water line - LMWL). Evaporation from an open water body fractionates isotopes so that the
54 remaining liquid phase is enriched in both ^2H and ^{18}O in proportion with their effective fractionation
55 factors accompanying this process. Consequently, the isotopic composition of the evaporating water
56 body evolves in the δ -space along the line known as the local evaporation line (LEL), whose slope is
57 significantly smaller than that characterising the local or global meteoric water lines. The position of
58 the isotopic composition of lake water along this line is strongly related to the water balance of the
59 lake (e.g. Gat, 1996; Gibson and Edwards, 2002; Rozanski et al., 2001).

60 The methodology of isotope-aided studies of the water balance of lakes has been thoroughly discussed
61 in a number of review papers and textbooks (e.g. Darling et al., 2005; Froehlich et al., 2005; Gat and
62 Bowser, 1991; Gat, 1995; Gonfiantini, 1986; Rozanski et al., 2001). Although several authors have
63 applied isotope techniques in studying lakes in cold climates (Gibson and Edwards, 2002; Gibson,

64 2002; Gibson et al., 1993; Jonsson et al., 2009; Turner et al., 2010; Yi et al., 2008), mostly in Canada
65 and northern Sweden, these studies were generally focused on lakes spread over large areas.

66 The central aim of this study was to quantify the groundwater dependence of 67 kettle lakes and ponds
67 situated across a relatively small area (90 km²) of the Rokua esker aquifer occupying a large
68 glaciofluvial deposit in northern Finland. To quantify the extent of the interaction between the aquifer
69 and the lakes, a dedicated isotope study was launched in 2013. This was part of comprehensive
70 investigations (2010-2012) aimed at understanding the hydrology of an esker aquifer area where some
71 of the kettle lakes and ponds have suffered from water level decline or eutrophication. Since the
72 seasonal isotopic behaviour of the selected lakes in the study area was already fairly well understood
73 based on the data collected from 2010 to 2012, it was decided to conduct a large-scale one-time survey
74 of the isotopic composition of all 67 lakes on the Rokua esker in order to quantify their dependence
75 on groundwater. Ala-aho et al. (2013), who studied 11 lakes on the esker, showed that the water levels
76 in closed-basin seepage lakes have more fluctuations than the drainage lakes, which have more stable
77 water levels. On the other hand, the drainage lakes are more productive. Their study also showed that
78 subsurface flow can transport phosphate to lakes. Therefore, it was important to quantify the
79 groundwater dependence of all lakes on the esker and propose an appropriate index reflecting this
80 dependence. The large-scale field campaign conducted in July and August 2013 comprised the
81 sampling of water in all 67 lakes for isotope analyses, combined with continuous temperature
82 measurements and aerial thermal imaging of the lakes.

83

84 **2. The study area**

85 The Rokua esker aquifer area, situated in Northern Finland, was formed during the transition period
86 from Late Glacial to Holocene, between approximately 12,000 and 9,000 years ago (Tikkanen, 2002).
87 As ice retreated, a long ridge formation, consisting mainly of fine and medium sand (Pajunen, 1995),
88 was shaped. Ancient sea banks surrounding the esker show that the esker was originally an island that
89 gradually rose from the sea (Aartolahti, 1973). Today, the highest elevation of the esker is 100 m
90 above the surrounding low-lying peatlands and the layer thickness of sand ranges from 30 m to more
91 than 100 m above the bedrock. Sea banks, dunes and kettle holes form a rolling and geologically
92 unique terrain (Aartolahti, 1973). Kettle holes were formed when ice blocks were buried in the ground
93 and, as they melted, left depressions in the landscape. The ground surface of the esker is mainly
94 lichen-covered pine forests. Hydrologically, the Rokua esker is an unconfined aquifer, one of the

95 largest in Finland, and it has two regional groundwater mounds (Rossi et al., 2014). The recharge area
96 of the aquifer is 90 km² and the discharge zones are situated in the surrounding peatlands, which
97 partially confine the aquifer (Rossi et al., 2012).

98 Kettle holes – long and narrow depressions – give Rokua esker its distinct character. The sizes of
99 these kettle holes vary. They can be 1 to 80 m deep, between 10 m and 1.5 km long, and 0.4 km wide
100 (Aartolahti, 1973). Most of the kettle holes are now dry, but due to the influence of groundwater in
101 the past, peat has accumulated at the bottom of them, creating kettle hole mires (Pajunen, 1995).
102 However, the alternating topography of the area is reflected in the existence of approximately 90
103 lakes or ponds, referred to as kettle lakes or ponds. Peat started to accumulate in the border regions
104 of the lakes more than 8,000 years ago, so most of the kettle lakes and ponds are partly paludified
105 (Pajunen, 1995). Nevertheless, the majority of the lakes and ponds are characterised by their crystal
106 clear water, which attract people; number of holiday homes and hotels are located on the lakeshores.
107 The lakes are nowadays widely used for different recreational activities, such as swimming, fishing
108 and scuba diving (Anttila and Heikkinen, 2007). The uniqueness of the glaciofluvial formation of
109 Rokua, in which the actions of ice, water and wind can be seen, has been recognised in many ways.
110 Some of the Rokua esker is protected by Natura 2000 and by the Finnish nature reserve network.
111 Rokua was recently chosen to be part of the UNESCO GeoPark Network and is currently the
112 northernmost region in this network.

113

114 **3. Materials and methods**

115 **3.1. Hydrological measurements and thermal imaging**

116 During 2010-2012, 11 lakes, 13 piezometers and 11 streams were sampled in the study area four times
117 per year to analyse the stable isotopic composition of water, nutrients, water quality parameters (T,
118 pH, E.C., O₂) and geochemical parameters (silica, major cations and anions) (Fig. 1). During the field
119 campaign conducted in July and August 2013, a total of 67 lakes and ponds were surveyed for the
120 same parameters and thermal images of lakes taken from the air in a helicopter using a FLIR thermal
121 camera. In addition, composite (monthly) precipitation samples were collected during the open water
122 season at the station on the esker during 2010-2013. Precipitation samples for winter were collected
123 once a year before snowmelt by taking a uniform sample of the whole snowpack depth.

124 Water quality parameters were analysed in the field using WTW Multi 3430 or Multi 350i meters for
125 temperature, oxygen, EC and pH. Samples of lake water were collected with a Limnos sampler,

126 approximately 1 m below the water surface and 1 m above the bottom of the lake. If the depth of the
127 lake was less than 2 m, only one sample from the depth of 1 m was taken and if it was more than 20
128 m, samples were taken from the middle of the water profile as well. Depending on their shape and
129 size, the lakes had between 1 and 4 sampling locations. Stream samples were collected by submerging
130 a bottle in water, facing upstream. Piezometers were pumped for at least 10 minutes prior to taking
131 groundwater samples or until the colour of the water was clear. The samples were collected one metre
132 below the water table. All sampling bottles (HDPE) were rinsed with the sampled water prior to
133 filling. Samples for isotope analyses were stored in the dark at a reduced temperature ($4\text{ }^{\circ}\text{C} \pm 2\text{ }^{\circ}\text{C}$).

134 The isotopic composition of water samples was analysed using CRDS technology with a Picarro
135 L2120-i analyser. Samples with visible colour or suspended matter were filtered (pore size $25\text{ }\mu\text{m}$)
136 prior to analysis. The measured $^2\text{H}/^1\text{H}$ and $^{18}\text{O}/^{16}\text{O}$ isotope ratios are reported as relative deviations
137 from the VSMOW standard. Typical uncertainty of the reported $\delta^{18}\text{O}$ and $\delta^2\text{H}$ values are $\pm 0.1\text{ }‰$ and
138 $\pm 1.0\text{ }‰$ respectively.

139 Lake water temperature was measured continuously during the ice-free period in 2013 for two lakes
140 on the Rokua esker: Ahveroinen (3.3 ha) and Saarinen (15.3 ha). Hobo loggers (pendant temperature
141 data logger UA-001-08 and conductivity logger U24-001, accuracy $0.1\text{ }^{\circ}\text{C}$) were installed 50 cm
142 below the lake surface. In addition, the surface water temperature for lake Oulujärvi (92800 ha) was
143 obtained from the database of the Finnish Environmental Institute (2013). Lake Oulujärvi is located
144 east, next to the study site, 1 km from the easternmost lake studied. Thermal imaging of the lakes was
145 conducted on 5 August 2013 using a Flir Thermacam P-60 thermal camera. This camera had $320 \times$
146 240 pixel sensor resolution and an opening of 24 ° . It covered the electromagnetic spectrum from 7.5
147 to $13\text{ }\mu\text{m}$. The imaging was taken by helicopter 150 meters above the lakes. The image data were
148 correlated to the predominant weather conditions (temperature and relative humidity) with data from
149 the FMI Pelso weather station measured every 10 minutes.

150 Depth profiling was undertaken in the lakes for which no depth contour lines are available (National
151 Land Survey of Finland, 2010a). It was carried out with a portable depth-sounding radar (resolution
152 0.1 m) or with a measuring cable and GPS system. Typically, two profiles from the shore to the
153 deepest point were defined. The number of measurement points differed between the lakes depending
154 on their size. In total, 52 lakes were surveyed.

155

156

157 3.2. Lake volumes

158 The volumes of the lakes were determined in an ArcGIS environment using depth profiling
159 measurements, contour lines and border lines. The water surface levels of the lakes were estimated
160 using elevation levels presented in the basic map (National Land Survey of Finland, 2010a). Lake
161 morphology was mostly interpolated using spline that results in a smooth surface passing by all the
162 input points (ESRI, 2014). The Tension method with 0.1 weight and 3 input points was used to
163 calculate the values for the interpolated cells. Interpolation rasters were extracted by surface water
164 areas. The mean depths of these new rasters were multiplied by the water surface areas in order to
165 calculate the volumes of the lakes.

166

167 3.3. Evaporation from lakes

168 Evaporation (E) was calculated individually for all the lakes surveyed using a mass transfer approach
169 (Rosenberry et al., 2007; Dingman, 2008). This method was chosen because it yields instantaneous
170 rates of evaporation and takes into account lake sizes (Harbeck, 1962). Our data enabled the
171 calculations of daily mean values of evaporation flux for all the lakes studied. Averaging the
172 parameters for periods of time longer than one day can lead to significant biases in the calculated E
173 values since on these time scales the vapour pressure differences and wind speed may correlate
174 (Jobson, 1972). The following expression was used to calculate the evaporation flux (Dingman,
175 2008):

$$176 E = K_E \cdot v_a \cdot (e_s - e_a), \quad (1)$$

177 where:

178 E is evaporation rate (mm s^{-1})

179 K_E is the mass-transfer coefficient in $\text{m km}^{-1} \text{kPa}^{-1}$ describing the impact of turbulent eddies of the
180 wind on vertical transport of water vapour from the lake with area A_L (km^2), $K_E = 1.69 \cdot 10^{-5} \cdot$
181 $A_L^{-0.05}$ (Harbeck, 1962)

182 v_a is wind speed (m s^{-1}) at 2 m height

183 e_s is the saturation vapour pressure in kPa at surface water temperature T_s ($^{\circ}\text{C}$), $e_s = 0.611 \cdot$
184 $\exp\left(\frac{17.3 \cdot T_s}{T_s + 237.3}\right)$

185 e_a is the vapour pressure in the air in kPa, $e_a = h \cdot 0.611 \cdot \exp\left(\frac{17.3 \cdot T_a}{T_a + 237.3}\right)$, where h is relative humidity
186 and T_a is air temperature ($^{\circ}\text{C}$).

187 Wind speed measured at 10 m height was adjusted to the corresponding speed at 2 m height using the
188 power law profile (Justus and Mikhail, 1976):

$$189 \quad v_z = v_r \left(\frac{z}{z_r}\right)^\beta, \quad (2)$$

190 where v_r is the measured wind speed at the reference height z_r (10 m), z is the height for which speed
191 is adjusted (2 m) and β is the friction coefficient. The value of 0.15 for β , characteristic for grassland,
192 was employed in our study (0.1 characterizes oceans and lakes) (Bañuelos-Ruedas et al., 2010) since
193 the lakes are surrounded by forests lowering the wind speed.

194 The meteorological parameters necessary for the calculations (relative humidity, wind speed and air
195 temperature) were obtained from the meteorological station 5502 (Vaala-Pelso) of the Finnish
196 Meteorological Institute (2014), located approximately 10 km from the site. A probable range for the
197 lakes' surface water temperature was evaluated using continuous temperature measurements at 50 cm
198 depth from one of the studied lakes, Ahveroinen (see section 4.1), and a standard deviation of this
199 temperature determined from thermal images. Using the derived temperature range, a probable range
200 for evaporation rates from all the lakes was calculated. The adopted method relies only on temperature
201 difference measured on one day, but since all the lakes are in a relatively small area with almost
202 identical weather conditions, it is highly probable that the seasonal behaviour of the surface water
203 temperature of the studied lakes is similar.

204

205 **3.4. Isotope mass balance**

206 Instantaneous water and isotope balances for an evaporating surface water body can be formulated as
207 follows:

$$208 \quad \frac{dV}{dt} = I_{TOT} - E - O_{TOT} \quad (3)$$

$$209 \quad \delta_L \frac{dV}{dt} + V \frac{d\delta_L}{dt} = \delta_{IT} \cdot I_{TOT} - \delta_E \cdot E - \delta_{OT} \cdot O_{TOT} \quad (4)$$

210 where V stands for the volume of the surface water body, δ_L signifies its isotopic composition and
211 I_{TOT} , E and O_{TOT} represent the total inflow, evaporation and total outflow of water from the system,
212 respectively, whereas δ_{IT} , δ_E and δ_{OT} stand for their respective isotopic compositions, expressed in
213 ‰. As the total inflow may consist of several components (precipitation, underground and surface
214 inflows), each with its specific isotopic composition, δ_{IT} should be calculated as a flux-weighted mean
215 of the respective isotopic compositions of individual components. The total outflow may also consist

216 of surface and underground components. For well-mixed systems it is typically assumed that $\delta_{OT} =$
 217 δ_L .

218 The isotopic composition of the evaporation flux, δ_E , cannot be measured directly. However, it can
 219 be calculated using the expression derived from the linear resistance model describing isotope effects
 220 accompanying evaporation process (Craig and Gordon, 1965; Horita et al., 2008):

$$221 \quad \delta_E = \frac{(\delta_L/\alpha_{LV}) - h_N \cdot \delta_A - \varepsilon}{(1 - h_N) + \Delta\varepsilon \cdot 10^{-3}} \quad (5)$$

222 where ε is the total effective isotope fractionation, $\varepsilon = \varepsilon^* + \Delta\varepsilon$, where ε^* stands for equilibrium isotope
 223 enrichment ($\varepsilon^* = (1 - 1/\alpha_{LV}) \cdot 10^3$) expressed in ‰ and α_{LV} represents the equilibrium isotope
 224 fractionation factor between liquid and gaseous phases. The kinetic isotope enrichment $\Delta\varepsilon$, is defined
 225 as $\Delta\varepsilon = C_k(1 - h_N)$ where C_k stands for the kinetic enrichment parameter. δ_A represents the isotopic
 226 composition of atmospheric water vapour over the evaporating water body (‰) and h_N is the relative
 227 humidity of the local atmosphere, normalized to the temperature of evaporating water.

228 When the evaporating water body is in hydrologic and isotopic steady-state ($dV/dt=0$ and $d\delta_L/dt=0$,
 229 respectively), the following approximate expression describing the isotope enrichment of the
 230 evaporating water body can be derived from eqs. 3-5 (see e.g. Gat and Bowser, 1991):

$$231 \quad \Delta\delta = \delta_{LS} - \delta_{IT} \cong \frac{\delta_A - \delta_{IT} + \varepsilon/h_N}{1 + \frac{I_{TOT} \cdot 1 - h_N}{E \cdot h_N}} \quad (6)$$

232 where $\Delta\delta$ stands for the evaporative enrichment and δ_{LS} is the steady-state isotopic composition of
 233 the studied system. The following expression describing the ratio of the total inflow to the evaporation
 234 rate can be derived from eq. (6):

$$235 \quad \frac{I_{TOT}}{E} = \frac{\delta_A - \delta_{LS} + \varepsilon/h_N}{(\delta_{LS} - \delta_{IT}) \frac{1 - h_N}{h_N}} \quad (7)$$

236 If the evaporation flux E can be assessed independently, as is the case of this study, the total inflow
 237 of water to the given lake can be calculated from eq. (7). From this, the groundwater component of
 238 this inflow can be further inferred, provided that the other components of this inflow are known or
 239 can be independently assessed.

240 To quantify the water balance of a lake with the aid of eq. (7) the knowledge of the isotopic
 241 composition of atmospheric moisture interacting with the lake, δ_A , is required. Field measurements
 242 of this parameter become feasible only recently thanks to advancements of CRDS technology.

243 However, the combined studies of the isotopic composition of atmospheric water vapour and
244 precipitation performed in moderate climates (Jacob and Sonntag, 1991; Schoch-Fischer et al., 1984)
245 have shown that, on monthly basis, the isotopic composition of precipitation is generally in isotopic
246 equilibrium with the local atmospheric moisture at ground-level temperature. This is particularly true
247 for summer season. Therefore, the value of δ_A can be derived from the isotopic composition of local
248 precipitation, δ_P , which is also required to quantify the isotopic composition of the total inflow to the
249 studied lake, δ_T , appearing in eq. (7). The following relation can be used to calculate δ_A (in ‰):

$$250 \quad \delta_A = \frac{1}{\alpha_{LV}} (\delta_P + 10^3) - 10^3 \quad (8)$$

251 Equation (7) is valid under two basic assumptions: (i) the evaporating water body is in hydrologic
252 and isotopic steady-state, and (ii) the water body is isotopically homogeneous. Natural surface water
253 systems, such as lakes, typically operate close to their hydrologic and isotopic steady-states attained
254 in the course of their long history. Their steady-state characteristics are defined by local climate,
255 morphological setting and prevailing hydrological regime. Such systems usually exhibit seasonal
256 fluctuations of varying amplitude, caused by seasonal fluctuations of local climate (surface air
257 temperature, relative humidity, precipitation amount), superimposed on long-term trends. Seasonal
258 ice-cover, typical for mid and high latitudes, may also contribute to the seasonal fluctuations of the
259 steady-state characteristics of such systems. The gradual attainment of the isotopic steady-state,
260 which is characterized by an exponential function describing the temporal evolution of δ_L , can be
261 observed only for surface water systems which are artificially created, such as dredging lakes
262 resulting from exploitation of gravel deposits (Zimmerman, 1979). The time constant characterizing
263 the dynamics of this process is mainly controlled by the mean turnover time of water in this system,
264 defined as the ratio of its volume to the total inflow, its hydrological balance (I_{TOT}/E ratio) and the
265 normalized relative humidity (e.g. Gonfiantini, 1986; Zimmerman, 1979).

266

267 **4. Results and discussion**

268 **4.1. Climate and lake water temperature data**

269 The climate is strongly seasonal in the Rokua esker study area. The long-term monthly mean values
270 of surface air temperature vary from -10.9 °C (January) to 13.2 °C (June) for the period between 1959
271 and 2013 (Fig. 2). The amount of monthly precipitation varies from 29 mm (February and April) to
272 79 mm (August) for the same period. The warmest months of the year are June, July and August. The

273 long-term (1970-2013) monthly mean relative humidity of air varies from 61 % (May) to 91 %
274 (November).

275 The seasonal temperature patterns of the monitored lakes were very similar, despite significant
276 differences in lake size (Fig. 3). Thus the surface water temperature of lake Ahveroinen 1 (mean value
277 of 19.1 °C) during the period from 1 June 2013 to 31 August 2013 was used as a basis for estimating
278 the water temperature of other lakes. Thermal images collected on 5 August 2013 yielded comparable
279 surface water temperatures that ranged from 19.5 °C to 24.6 °C, with a mean of 21.3 °C and a standard
280 deviation of 0.87 °C. Combining the results of continuous temperature measurements and thermal
281 images, an estimate of the mean surface water temperature of all lakes for the period from 1 June to
282 31 August 2013 was derived to be $19.10 \text{ °C} \pm 0.87 \text{ °C}$. This temperature was used in the isotope mass
283 balance calculations.

284

285 **4.2. Local isotopic compositions**

286 An overview of the isotopic composition of different types of water in the study area is presented on
287 the $\delta^2\text{H}$ - $\delta^{18}\text{O}$ space in Fig. 4. It comprises precipitation data collected during the period from 18
288 March 2010 till 29 October 2013 at the station located on the esker, the mean isotopic compositions
289 of the selected lakes, streams and groundwater monitored during the period 2010-2013 (Table 1), as
290 well as the isotopic compositions of 67 lakes surveyed in July and August 2013 (Table 2).

291 The local meteoric water line (LMWL) of Rokua ($\delta^2\text{H} = 7.77 \cdot \delta^{18}\text{O} + 9.55$) was defined using the δ
292 values of precipitation samples collected during the years 2010-2013 (Fig. 4). The local evaporation
293 line (LEL), $\delta^2\text{H} = 5.09 \cdot \delta^{18}\text{O} - 28.19$, is the best fit line of the δ values representing lake water data
294 for the year 2013. The intercept of the LMWL and LEL lines (-14.1 ‰ and -100 ‰ respectively),
295 yields the estimate of the total water inflow to the studied lakes (δ_{T}), which consists of direct
296 precipitation input as well as possible groundwater and surface water input. Slightly elevated mean
297 $\delta^{18}\text{O}$ and $\delta^2\text{H}$ values of local groundwater (-13.1 ‰ and -95 ‰), combined with reduced deuterium
298 excess ($d = \delta^2\text{H} - 8 \cdot \delta^{18}\text{O} = 4.8 \text{ ‰}$) when compared to deuterium excess of precipitation (12.8 ‰),
299 indicate the presence of an evaporation signal in the local groundwater. Furthermore, some of the
300 winter precipitation is most probably returned to the atmosphere via sublimation and does not
301 contribute to groundwater recharge.

302 Although majority of groundwater samples cluster near the LMWL-LEL intersect, there are some
303 data points lying along the LEL in the $\delta^{18}\text{O}$ - $\delta^2\text{H}$ plot indicating the contribution of (evaporated) lake

304 water to groundwater. However, the interconnection between the lakes via groundwater is likely to
305 be minor since lakes probably have groundwater table maxima between them as they are situated in
306 deep holes in the landscape. Nevertheless, the existence of deeper flow paths from the upper elevation
307 lakes to the lower ones cannot be excluded. Based on the estimation of elevation differences and
308 distances between the lakes, we identified the lakes which do not have surface inflows but which
309 might receive some groundwater input originating from upper elevation lakes. These are lakes No. 6,
310 14, 20, 34, 38, 41, 47, 50 and 59. The sensitivity study presented in section 4.5 considers probable
311 changes of the isotopic composition of the total inflow to each lake caused by the presence of
312 evaporated lake water component.

313 The influence of evaporated lake water seeping to groundwater is illustrated in Fig. 5, showing the
314 isotopic composition of lake Ahveroinen 1 and adjacent groundwater. The mean $\delta^{18}\text{O}$ and $\delta^2\text{H}$ values
315 of piezometers MEA 2010 and MEA 1907 situated on the south-eastern and north-western sides of
316 the lake were -13.4‰ and -97‰ and -10.7‰ and -83‰ respectively, clearly indicating a
317 substantial (ca. 55 %) contribution of lake water to groundwater at the north-western side of the lake.
318 A smaller contribution (ca. 10 %) of lake water to groundwater can be seen on the eastern and western
319 sides of the lake where the mean $\delta^{18}\text{O}$ and $\delta^2\text{H}$ values of groundwater were -12.9‰ and -93‰
320 respectively. The main direction of groundwater flow is therefore from south-east to north-west,
321 which coincides with the results from seepage measurements conducted by Ala-aho et al. (2013). The
322 direction of groundwater flow can also be noted from the difference in the mean isotopic composition
323 of the lake water between points 2 and 3 of -8.7‰ and -73‰ and -8.5‰ and -72‰ respectively.
324 The difference in isotopic compositions between points 2 and 3 was greatest during the winter: in
325 March 2011 the difference in $\delta^{18}\text{O}$ and $\delta^2\text{H}$ between these points was -1.1‰ and -4‰ respectively.

326

327 **4.3. Temporal variations in the isotopic composition of lake water**

328 The seasonal variability in the isotopic composition of the lakes studied is illustrated in Fig. 6,
329 showing changes of $\delta^{18}\text{O}$ in lake Ahveroinen 1 at two depths (1 and 4 meters). $\delta^{18}\text{O}$ of lake
330 Ahveroinen 1 reveals distinct seasonal fluctuations with peak-to-peak amplitude in the order of 1 ‰.
331 This lake does not have any surface inflows or outflows. After the disappearance of ice cover during
332 the spring (April-May), the lake starts to evaporate, which results in its gradual enrichment in heavy
333 isotopes, approaching the steady-state value sometime in September-October. Freezing of the lake in
334 late autumn stops the evaporation flux. Systematic decline of $\delta^{18}\text{O}$ during ice-cover period seen in

335 Fig. 6 stems from gradual dilution of lake water with groundwater seeping into the lake. Figure 6
336 shows that the lake is well mixed throughout the year.

337 The declining parts of the $\delta^{18}\text{O}$ curve in Fig. 6 can be used to assess the intensity of groundwater
338 inflow during ice-cover period, if the volume of the studied lake is known and the isotopic
339 composition of groundwater is constant. The isotope balance of such lake system (eq. 4) can be then
340 expressed as follows:

$$341 \quad V \frac{d\delta_L}{dt} = \delta_{IT} \cdot I_{TOT} - \delta_{OT} \cdot O_{TOT} \quad (9)$$

342 Since $I_{TOT} = I_{GW}$, $\delta_{IT} = \delta_{GW}$, $O_{TOT} = O_{GW} = I_{GW}$ and $\delta_{OT} = \delta_L$, eq. (9) becomes:

$$343 \quad \frac{d\delta_L}{dt} = \frac{I_{GW}}{V} (\delta_{GW} - \delta_L) \quad (10)$$

344 The solution of this differential equation reads as follows:

$$345 \quad \delta_L = (\delta_{L0} - \delta_{GW}) \cdot e^{-k \cdot t} + \delta_{GW} \quad (11)$$

346 where $k = I_{GW}/V$ and δ_{L0} is the isotopic composition of the lake at the beginning of ice-cover period
347 ($\delta^{18}\text{O}_{L0} = -8.5 \text{ ‰}$ for lake Ahveroinen 1).

348 Equation (10), with $\delta_L = \delta_{L0}$, can be used to calculate the mean flux of groundwater to the lake during
349 ice-cover period. The observed reduction of $\delta^{18}\text{O}$ of lake Ahveroinen 1 by ca. 1.2 ‰ over the six-
350 month period (cf. Fig. 6, Table 1) results from the continuous inflow of groundwater with specific
351 isotopic signature ($\delta^{18}\text{O}_{GW} = -13.4 \text{ ‰}$). The groundwater seepage rate obtained from eq. (12) is ca.
352 $160 \text{ m}^3 \text{ day}^{-1}$. Identical value was obtained using corresponding ^2H data. It is worth noting that
353 groundwater inflow to lake Ahveroinen 1, derived for the summer period of 2013 from isotope mass
354 balance calculations (ca. $300 \text{ m}^3 \text{ day}^{-1}$) is almost two times higher, which suggests significant seasonal
355 variations of groundwater inflow to Rokua lakes, with high groundwater fluxes during summer and
356 low fluxes during winter. These variations most probably stem from seasonal fluctuations of water
357 table caused mainly by snow melt induced groundwater recharge in spring. Observations for lake
358 water stage and adjacent piezometer MEA 2010 (cf. Fig. 5) during two years demonstrated an average
359 20 % higher hydraulic gradient in the summer than in the winter. This is in agreement with our data
360 showing higher groundwater inflow during summer. The annual variability in groundwater fluxes to
361 lakes in the study area was also showed in a modelling study by Ala-aho et al. (2015).

363 4.4. Quantifying groundwater dependence of the studied lakes

364 Out of 67 Rokua lakes sampled during July-August 2013 field campaign, 50 lakes do not reveal any
365 surface water inflow in the form of a stream or a creek. For the remaining 17 lakes surface inflows
366 were identified. For all but one lake those surface inflows could be linked to specific upstream lakes
367 which were sampled during the July-August 2013 campaign.

368 The isotopic composition of the lakes sampled covers a wide range of δ values: from -5.6‰ to -12.7
369 ‰ and from -57‰ to -93‰ for $\delta^{18}\text{O}$ and $\delta^2\text{H}$ respectively. This large variability reflects a wide
370 spectrum of the heavy isotope enrichment of the lakes studied. Since Rokua lakes are situated in a
371 unique climatic region, their observed isotopic composition is primarily controlled by their water
372 balance, which in turn can be characterised by the total inflow-to-evaporation ratio.

373 Equation (7) was used to calculate the total inflow-to-evaporation ratios (I_{TOT}/E) for all studied lakes.
374 The isotope mass balance calculations were run for the period of June-August 2013 separately for
375 ^{18}O and ^2H . Since the evaporation rates from the studied lakes were derived from eq. (1),
376 independently of any mass balance considerations, the total inflow to each lake could also be
377 calculated from the assessed I_{TOT}/E ratios.

378 The values of the parameters occurring in eq. (7) were derived as follows:

379 (i) The mean isotopic composition of atmospheric moisture (δ_A) was calculated with the eq. (8)
380 using the available isotope data for local precipitation. The following mean δ_A values were used in
381 isotope mass balance calculations: $\delta^{18}\text{O}_A = -20.4\text{‰}$ and $\delta^2\text{H}_A = -149\text{‰}$.

382 (ii) The mean relative humidity, normalized to lake water temperature (h_N) was calculated using the
383 mean surface air temperature ($+14.9\text{ °C}$), the mean surface water temperature of the lakes ($+19.1\text{ °C}$)
384 and the mean relative air-based humidity calculated on the basis of daily mean values available from
385 meteorological station in the area (79.2%). The resulting mean h_N value was 60.7% .

386 (iii) The total effective isotope fractionation (ϵ) was derived as the sum of the equilibrium and kinetic
387 isotope enrichments ($\epsilon = \epsilon^* + \Delta\epsilon$). The equilibrium isotope enrichment (ϵ^*) values for ^{18}O and ^2H ,
388 were calculated for the mean surface water temperature of $+19.1\text{ °C}$ using the known temperature
389 dependence of the empirical equilibrium fractionation factors, α_{LV} (Horita and Wesolowski, 1994).
390 The values of kinetic enrichment parameters (C_k) used to calculate $\Delta\epsilon$, 14.2‰ for ^{18}O and 12.5‰
391 for ^2H , were adopted after Gonfiantini (1986). Those values were obtained in wind-tunnel
392 experiments (Vogt, 1976) and are widely used in lake studies.

393 (iv) Isotopic homogeneity of the studied lakes was addressed through multiple samplings of large
394 lakes (in both horizontal and vertical direction - cf. section 3.1). The range of the measured $\delta^{18}\text{O}$
395 values for the given lake was generally lower than one per mil. It was assumed that the average values
396 calculated on the basis of individual measurements performed in each lake represent sufficiently well
397 the studied systems.

398 (v) The isotopic composition of lake water obtained during the sampling campaign in July and
399 August 2013 for each studied lake was used in the isotope mass balance calculations. As discussed
400 in section 3.4 above, the isotopic compositions of the studied lakes fluctuate seasonally reaching their
401 steady-state values toward the end of ice-free period (September-October). Therefore, the isotopic
402 compositions of lake water samples collected during the late summer (July-August) may still deviate
403 slightly from the respective steady-state values, thus creating uncertainty in the assessed components
404 of the water (see section 4.5).

405 (vi) As the isotopic compositions of the surface and underground components of water inflow to each
406 studied lake were not measured directly, an iterative approach was adopted to calculate δ_{T}
407 individually for each lake. In the first step it was assumed that δ_{T} is defined by the intercept of the
408 LMWL and LEL lines (Fig. 4). With these δ_{T} values the underground component of I_{TOT} for each
409 lake was derived from eq. (7). The second step differed for the lakes without surface inflow and with
410 identified surface inflow from an upstream lake. For the lakes without surface inflow the δ_{T} values
411 were calculated individually as flux-weighted averages of the underground inflow obtained in the
412 first/previous step of the procedure and precipitation input to the given lake, each with their respective
413 mean isotopic compositions representing the period of June-August 2013 (cf. section 4.2 above). For
414 the lakes with identified surface inflow from an upstream lake, in the first instance the total outflow
415 of water from the upstream lake was calculated using appropriate mass balance equation. Then, it
416 was assumed that 25 % of the total outflow from the upstream lake flows to the downstream lake as
417 surface inflow carrying the isotopic composition characteristic for the upstream lake. The δ_{T} values
418 were calculated individually for each lake belonging to this group of lakes as flux-weighted averages
419 of three components: precipitation, surface inflow and groundwater inflow. For both lake groups the
420 calculations were repeated until the change of δ_{T} in subsequent iteration step was in the order of the
421 analytical uncertainty of isotope measurements (0.1 ‰ for $\delta^{18}\text{O}$ and 1 ‰ for $\delta^2\text{H}$).

422 The calculated inflow-to-evaporation ratios of the studied lakes based on ^{18}O isotope mass balance
423 are shown in Fig. 7 as a function of isotope enrichment of lake water with respect to the isotopic
424 composition of the total inflow to the given lake. They vary in a wide range, from I_{TOT}/E values

425 between 2 and 3 and large ^{18}O isotope enrichments between approximately 6.5 and 8.0 ‰, indicating
426 evaporation dominated systems, to typical through-flow lakes characterized by I_{TOT}/E ratios higher
427 than 10 and moderate ^{18}O isotope enrichments of less than 2 ‰ (Table 2). Knowing the volume and
428 the total inflow, the mean turnover time of water (MTT) in each lake could be quantified as the ratio
429 of lake volume to the total inflow. The calculated MTT values range from approximately one week
430 for the Pasko pond ($V = 2 \times 10^3 \text{ m}^3$, mean depth 0.2 m, maximum depth 0.7 m) to approximately five
431 years for lake Saarijärvi 2 ($V = 2.47 \times 10^6 \text{ m}^3$, mean depth 11.8 m, maximum depth 26 m), with the
432 mean in the order of ten months (Table 2). Lake Saarijärvi 2 is the deepest of all the lakes surveyed.
433 As expected, the calculated MTT values correlate well with the mean depth of the studied lakes,
434 expressed as the volume-to-surface area ratio. However, the link between MTT and the I_{TOT}/E ratio
435 is much weaker; lakes with higher I_{TOT}/E ratios tend to have shorter mean turnover times.

436 The dependence of the studied lakes on groundwater can be quantified through an index (G index)
437 defined as the percentage contribution of groundwater inflow to the total inflow of water to the given
438 lake. Groundwater inflow was derived by subtracting the precipitation and surface water inflow (if
439 exists) from the total inflow. Such an evaluation was undertaken for all the lakes listed in Table 2.
440 Note that for the group of lakes with identified surface inflow from an upstream lake it was assumed
441 arbitrarily that this surface inflow is 25 % of the total outflow from the upstream lake (discharges of
442 surface inflows were not measured). The resulting groundwater seepage rates vary from less than 20
443 $\text{m}^3\text{day}^{-1}$ for Kissalampi pond to around $14 \times 10^3 \text{ m}^3\text{day}^{-1}$ for lake Nimisjärvi, the lake with the largest
444 surface area (167.5 ha) among all studied lakes.

445 Figure 8 summarises the values of G index obtained for the lakes surveyed during the July-August
446 2013 sampling campaign. The mean values of G index obtained from ^2H and ^{18}O balance are shown.
447 They vary from ca. 40 % to more than 95 %. The lowest value (39.4 %) was obtained for lake Etu-
448 Salminen. The highest G values were derived for lakes Kiiskeroinen (97.1 %) and Levä-Soppinen
449 (97.5 %). Interestingly, these lakes are characterised by a high degree of eutrophication induced by
450 high loads of phosphorus brought to the lakes with groundwater (Ala-aho et al. 2013). Although the
451 G index describes groundwater dependency of the studied lakes rather unambiguously, also lakes
452 with moderate G index values can suffer if groundwater table in the esker aquifer would decline as a
453 result of climate and/or land-use changes.

454 The isotope mass balance calculations for Rokua lakes were run independently for ^{18}O and ^2H data.
455 Consistent results were obtained with respect to three evaluated elements of lake water balance

456 (I_{TOT}/E ratios, MTT values and the G index) reported in Table 2. These quantities, derived
457 independently from ^2H -based and ^{18}O -based isotope mass balances are highly correlated ($R^2 = 0.9681$,
458 0.9972 and 0.9745 for I_{TOT}/E ratios, MTT values and the G index, respectively). The total inflow-to-
459 evaporation ratios derived from ^{18}O -based balance turned out to be ca. 10.8 % higher on the average
460 than those derived from ^2H -based balance. For the G index this difference is approximately 2.3 %.
461 The MTT values were ca. 12.5 % higher for ^2H -based balance.

462 Small but significant differences in the values of the evaluated quantities (I_{TOT}/E ratios, MTT, G
463 index), derived independently from ^{18}O - and ^2H -based isotope mass balance calculations, stem most
464 probably from their different sensitivity to small changes of the measurable parameters (air and lake
465 water temperature, relative humidity, isotopic composition of local precipitation, isotopic
466 composition of lake water) rooted in different role of equilibrium and kinetic fractionation during the
467 evaporation process. While for ^{18}O the ratio of equilibrium to kinetic isotope fractionation is in the
468 order of one, for ^2H it is ten times higher. Since isotope mass balance method relies on isotope
469 enrichment of lake water along the local evaporation line, controlled mostly by kinetic fractionation,
470 the ^{18}O -based balance calculations are generally considered more reliable (e.g. Rozanski et al., 2001).

471

472 **4.5. Uncertainty assessment**

473 The above methodology for quantifying elements of water balance in the lakes studied introduces
474 some uncertainties linked to the assumptions made and the uncertainties associated with the
475 parameters used in the evaluation process. Sensitivity tests were performed to derive the range of
476 uncertainties associated with the quantities being evaluated, such as mean turnover time, total inflow-
477 to-evaporation ratio and the G index. The sensitivity analysis was focussing on eq. (7). All variables
478 present in this equation were considered in this process. The results for ^{18}O -based calculations are
479 summarized in Table 3.

480 The uncertainty with regard to lake water temperature was probed assuming the temperature change
481 of ± 0.87 °C (cf. section 4.1). The uncertainty of lake water temperature leads to uncertainty as regards
482 the evaporation flux, which in turn influences the I_{TOT}/E , MTT and G values derived for each lake.
483 Also equilibrium isotope enrichment is a function of temperature. The mean turnover time increases
484 by ca. 15 % when the temperature of the lake is reduced by 0.87 °C, and decreases by approximately
485 12 % when the temperature increases by the same amount. The G index reveals lower sensitivity (2.9

486 and 3.6 %, respectively). The smallest changes were obtained for I_{TOT}/E ratios (0.9 and 0.7 %,
487 respectively).

488 The changes of relative humidity of the atmosphere normalised to the temperature of the lake surface
489 have an impact on the evaporation flux, control the I_{TOT}/E ratios through eq. (7) and determine the
490 actual value of kinetic isotope enrichment $\Delta\epsilon$. It was assumed in the calculations that normalized
491 relative humidity changes by ± 2 %. As seen in Table 3, the resulting changes of the derived quantities
492 are moderate, the mean turnover time being the most sensitive parameter.

493 It is apparent from Table 3 that among isotope parameters occurring in eq. (7), the isotopic
494 composition of lake water (δ_{LS}) and the isotopic composition of the total inflow (δ_{IT}), are the two
495 most important variables in the isotope mass balance calculations. An increase of $\delta^{18}O_{LS}$ by 0.5 ‰,
496 which may account for possible departures from the isotopic steady-state of the investigated lakes
497 (cf. section 4.4), leads to decrease of calculated I_{TOT}/E ratios on the average by 15.8 %, increase of
498 MTT values by 19.6 % and decrease of G index values by 3.3 %. An increase of $\delta^{18}O_{IT}$ by 0.5 ‰,
499 which may result from the contribution of an evaporated lake water originating from an upstream
500 lake to groundwater input, leads to substantial increase of I_{TOT}/E ratios (20.2 % on the average),
501 comparable decrease of MTT values (14.8 % on the average) and moderate increase of the G index
502 (4.4 % on the average). Variation of the ^{18}O isotopic composition of atmospheric water vapour by \pm
503 1.0 ‰ introduces changes in the calculated elements of the water balance of the studied lakes in the
504 order of several per cent (Table 3).

505 Figure 9 shows the percentage changes of I_{TOT}/E ratios calculated for all studied lakes using eq. (7),
506 in response to the increase of δ_{LS} or δ_{IT} by 0.5 ‰. The sensitivity of the calculated I_{TOT}/E ratios to the
507 given increase of δ_{LS} or δ_{IT} raises sharply with increasing value of this parameter. This is particularly
508 true for through-flow systems characterized by high I_{TOT}/E ratios. Therefore, when isotope studies
509 aimed at quantifying water balance of such systems are planned, it is important to characterize these
510 two isotope quantities as good as reasonably possible.

511

512 **5. Conclusions**

513 The Rokua esker, with its numerous lakes located across a relatively small area, provided a unique
514 opportunity to explore the possibilities offered by environmental isotope techniques in quantifying
515 the water balances of lakes and their dependency on groundwater in a sub-polar climatic setting. The

516 quantification of groundwater seepages to lakes using conventional methods is notoriously difficult
517 and associated with considerable uncertainty. The presented study demonstrates the power of isotope
518 mass balance approach for resolving this issue. It appears that a stable isotope analysis of lake water
519 samples, collected at right time and supplemented by appropriate field observations, may lead to
520 quantitative assessment of the water balance of a large number of lakes located in a similar climatic
521 settings.

522 The presented study has demonstrated that consistent results are obtained when the isotope mass
523 balance calculations are run independently for oxygen-18 and deuterium. This strengthens the
524 position of heavy stable isotopes of water as a unique tool for quantifying elements of water balance
525 of lakes, particularly for groundwater-dominated systems. Solving three equations simultaneously
526 (one water balance equation plus two isotope balance equations) may help to quantify key balance-
527 related parameters such as evaporation and groundwater inflow and outflow rates for the studied lake
528 system, which are difficult to quantify using conventional methods.

529 The specific behaviour of lakes located in sub-polar regions, with their seasonal ice cover extending
530 over several months, offers another opportunity for quantifying groundwater seepage during ice-
531 cover periods. As shown in this study, observations of seasonal changes in the stable isotopic
532 composition of lake water, in particular during the ice-cover period, combined with the survey of
533 isotopic composition of groundwater in the vicinity of the lakes studied, allows the quantification of
534 groundwater fluxes to this lake during winter. If such an approach is combined with the isotope mass
535 balance calculations performed for ice-free summer season, important information about the seasonal
536 variability of groundwater seepage to lakes located in sub-polar and polar regions can be obtained.

537 The *G* index characterizing groundwater dependency of a lake proposed in this study, and defined as
538 a percentage contribution of groundwater inflow to the total inflow of water to the given lake, appears
539 to be a straightforward, quantitative measure of this dependency. The studied Rokua lakes appear to
540 be strongly dependent on groundwater; more than 40 % of water received by these lakes comes as
541 groundwater inflow. The quantitative evaluation of groundwater dependency of lakes via the *G* index
542 proposed in this study may assist lake restoration policies in areas where groundwater is a source of
543 nutrients to the studied lakes.

544 **Acknowledgements**

545 This work is funded by the 7th framework project GENESIS (226536), Renlund Foundation, Maa- ja
546 vesitekniikan tuki r.y, and the Academy of Finland, AKVA-programme. KR's contribution was partly
547 supported through the statutory funds of the AGH university of Science and Technology (project no.
548 11.11.220.01). We would like to thank Kirsti Korkka-Niemi and Anne Rautio from University of
549 Helsinki for their assistance with the thermal imaging.

550

551 **References**

- 552 Aartolahti, T.: Morphology, vegetation and development of Rokuanvaara, an esker and dune
553 complex in Finland, *Soc. Geogr. Fenn.*, 127, 1–53, 1973.
- 554 Ala-aho, P., Rossi, P. M., Isokangas, E. and Kløve, B.: Fully integrated surface-subsurface flow
555 modelling of groundwater-lake interaction in an esker aquifer: Model verification with stable
556 isotopes and airborne thermal imaging, *J. Hydrol.*, 522, 391–406,
557 doi:10.1016/j.jhydrol.2014.12.054, 2015.
- 558 Ala-aho, P., Rossi, P. M. and Kløve, B.: Interaction of esker groundwater with headwater lakes and
559 streams, *J. Hydrol.*, 500, 144–156, doi:10.1016/j.jhydrol.2013.07.014, 2013.
- 560 Anttila, E.-L. and Heikkinen, M.-L.: Rokuan pinta- ja pohjavesien vedenkorkeudet ja niissä
561 tapahtuneet muutokset, in *Rokuan alueen järvet ja lammet*. North Ostrobothnia Regional
562 Environment Centre Reports 5 | 2007, edited by M.-L. Heikkinen and T. Väisänen, pp. 12–25,
563 North Ostrobothnia Regional Environment Centre, Oulu., 2007.
- 564 Bañuelos-Ruedas, F., Angeles-Camacho, C. and Rios-Marcuello, S.: Analysis and validation of the
565 methodology used in the extrapolation of wind speed data at different heights, *Renew. Sustain.*
566 *Energy Rev.*, 14(8), 2383–2391, doi:10.1016/j.rser.2010.05.001, 2010.
- 567 Belanger, T. V., Mikutel, D. F. and Churchill, P. A.: Groundwater seepage nutrient loading in a
568 Florida Lake, *Water Res.*, 19(6), 773–781, 1985.
- 569 Brock, T. D., Lee, D. R., Janes, D. and Winek, D.: Groundwater seepage as a nutrient source to a
570 drainage lake; Lake Mendota, Wisconsin, *Water Res.*, 16(7), 1255–1263, 1982.
- 571 Clark, I. D. and Fritz, P.: *Environmental isotopes in hydrogeology*, Lewis Publishers, New York.,
572 1997.
- 573 Craig, H.: Isotopic variations in meteoric waters, *Science*, 133(3465), 1702–3,
574 doi:10.1126/science.133.3465.1702, 1961.
- 575 Craig, H. and Gordon, L. I. .: Deuterium and Oxygen-18 Variations in the Ocean and the Marine
576 Atmosphere, in *Stable Isotopes in Oceanographic Studies and Paleotemperatures*, edited by E.
577 Tongiorgi, pp. 9–130, Laboratorio di geologia nucleare, Pisa., 1965.
- 578 Darling, W. G., Bath, A. H., Gibson, J. J. and Rozanski, K.: Isotopes in water, in *Isotopes in*
579 *palaeoenvironmental research*, edited by M. J. Leng, pp. 1–66, Springer, Dordrecht., 2005.
- 580 Dinçer, T.: The use of oxygen 18 and deuterium concentrations in the water balance of lakes, *Water*
581 *Resour. Res.*, 4(6), 1289–1306, doi:10.1029/WR004i006p01289, 1968.
- 582 Dingman, S. L.: *Physical Hydrology*, 2. ed., Waveland press, Long Grove, IL., 2008.

583 EC: Directive 2006/118/EC of the European Parliament and of the Council on the protection of
584 groundwater against pollution and deterioration, Official Journal of the European Union, Brussels.,
585 2006.

586 ESRI: Applying a spline interpolation, [online] Available from:
587 http://webhelp.esri.com/arcgisdesktop/9.2/index.cfm?TopicName=Applying_a_spline_interpolation
588 , 2014.

589 Finnish Environmental Institute: Environmental information system (Hertta), Data downloaded 11
590 Novemb. 2013, Data downloaded 11 November 2013, 2013.

591 Finnish Meteorological Institute: Climate data from Vaala-Pelso meteorological station, , Data
592 received 28 January 2014, 2014.

593 Froehlich, K., Gonfiantini, R. and Rozanski, K.: Isotopes in lake studies: A historical perspective, in
594 Isotopes in the Water Cycle. Past, Present and Future of a Developing Science, edited by P. K.
595 Aggarwal, J. R. Gat, and K. F. O. Froehlich, pp. 139–151, Springer, 3300AA Dordrecht, The
596 Netherlands., 2005.

597 Gat, J. R.: Stable isotopes of fresh and saline lakes, in Physics and Chemistry of Lakes, edited by A.
598 Lerman, D. M. Imboden, and J. R. Gat, pp. 139–165, Springer-Verlag, Berlin., 1995.

599 Gat, J. R.: Oxygen and hydrogen isotopes in the hydrologic cycle, *Annu. Rev. Earth Planet. Sci.*,
600 24(1), 225–262, doi:10.1146/annurev.earth.24.1.225, 1996.

601 Gat, J. R.: Isotope hydrology: A study of the water cycle, Imperial College Press, London., 2010.

602 Gat, J. R. and Bowser, C.: The heavy isotope enrichment of water in coupled evaporative systems,
603 in *Stable Isotope Geochemistry: A Tribute to Samuel Epstein*, Special Publication No. 3, edited by
604 A. A. Levinson, pp. 159–169, The Geochemical Society, Calgary., 1991.

605 Gibson, J. J.: Short-term evaporation and water budget comparisons in shallow Arctic lakes using
606 non-steady isotope mass balance, *J. Hydrol.*, 264(1-4), 242–261, doi:10.1016/S0022-
607 1694(02)00091-4, 2002.

608 Gibson, J. J. and Edwards, T. W. D.: Regional water balance trends and evaporation-transpiration
609 partitioning from a stable isotope survey of lakes in northern Canada, *Global Biogeochem. Cycles*,
610 16(2), 10–1–10–14, doi:10.1029/2001GB001839, 2002.

611 Gibson, J. J., Edwards, T. W. D., Bursey, G. G. and Prowse, T. D.: Estimating Evaporation Using
612 Stable Isotopes : Quantitative Results and Sensitivity Analysis for Two Catchments in Northern
613 Canada, *Nord. Hydrol.*, 24, 79–94, 1993.

614 Gonfiantini, R.: Environmental isotopes in lake studies, in *Handbook of Environmental Isotope
615 Geochemistry*, Vol. 2. The Terrestrial Environment, edited by B. P. Fritz and J. C. Fontes, pp. 113–
616 168, Elsevier, Amsterdam., 1986.

- 617 Harbeck, G. E. J.: A practical field technique for measuring reservoir evaporation utilizing mass-
618 transfer theory, U.S. Geol. Surv. Prof. Pap., 272-E, p. 101–105, 1962.
- 619 Horita, J., Rozanski, K. and Cohen, S.: Isotope effects in the evaporation of water: a status report of
620 the Craig-Gordon model., *Isotopes Environ. Health Stud.*, 44(1), 23–49,
621 doi:10.1080/10256010801887174, 2008.
- 622 Horita, J. and Wesolowski, D.: Liquid-vapour fractionation of oxygen and hydrogen isotopes of
623 water from the freezing to the critical temperature, *Geochim. Cosmochim. Acta*, 58(16), 3425–
624 3437, doi:10.1016/0016-7037(94)90096-5, 1994.
- 625 Jacob, H. and Sonntag, C.: An 8-year record of the seasonal variation of ²H and ¹⁸O in atmospheric
626 water vapour and precipitation in Heidelberg, Germany, *Tellus*, 43B, 291–300, doi:10.1034/j.1600-
627 0889.1991.t01-2-00003.x, 1991.
- 628 Jobson, H. E.: Effect of using averaged data on the computed evaporation, *Water Resour. Res.*,
629 8(2), 513–518, 1972.
- 630 Jonsson, C. E., Leng, M. J., Rosqvist, G. C., Seibert, J. and Arrowsmith, C.: Stable oxygen and
631 hydrogen isotopes in sub-Arctic lake waters from northern Sweden, *J. Hydrol.*, 376(1-2), 143–151,
632 doi:10.1016/j.jhydrol.2009.07.021, 2009.
- 633 Justus, C. G. and Mikhail, A.: Height variation of wind speed and distribution statistics, *Geophys.*
634 *Res. Lett.*, 3(5), 261–264, doi:10.1029/GL003i005p00261, 1976.
- 635 Kidmose, J., Nilsson, B., Engesgaard, P., Frandsen, M., Karan, S., Landkildehus, F., Søndergaard,
636 M. and Jeppesen, E.: Focused groundwater discharge of phosphorus to a eutrophic seepage lake
637 (Lake Væng, Denmark): implications for lake ecological state and restoration, *Hydrogeol. J.*, 21(8),
638 1787–1802, doi:10.1007/s10040-013-1043-7, 2013.
- 639 Kløve, B., Ala-aho, P., Bertrand, G., Boukalova, Z., Ertürk, A., Goldscheider, N., Ilmonen, J.,
640 Karakaya, N., Kupfersberger, H., Kværner, J., Lundberg, A., Mileusnić, M., Moszczynska, A.,
641 Muotka, T., Preda, E., Rossi, P., Siergieiev, D., Šimek, J., Wachniew, P., Angheluta, V. and
642 Widerlund, A.: Groundwater dependent ecosystems. Part I: Hydroecological status and trends,
643 *Environ. Sci. Policy*, 14(7), 770–781, doi:10.1016/j.envsci.2011.04.002, 2011.
- 644 Krabbenhoft, D. P., Bowser, C. J., Anderson, M. P. and Valley, J. W.: Estimating Groundwater
645 Exchange With Lakes 1 . The Stable Isotope Mass Balance Method, *Water Resour. Res.*, 26(10),
646 2445–2453, 1990.
- 647 National Land Survey of Finland: Basic map, 2010a.
- 648 National Land Survey of Finland: Digital elevation model, 2010b.
- 649 Pajunen, H.: Holocene accumulation of peat in the area of an esker and dune complex,
650 Rokuanvaara, central Finland, *Geol. Surv. Finland, Spec. Pap.*, 20, 125–133, 1995.

- 651 Rosenberry, D. O., Labaugh, J. W. and Hunt, R. J.: Use of monitoring wells , portable piezometers ,
652 and seepage meters to quantify flow between surface water and ground water, in *Field Techniques*
653 *for Estimating Water Fluxes Between Surface Water and Ground Water*, edited by D. O.
654 Rosenberry and J. W. LaBaugh, pp. 43–70, US Geological Survey, Unites States., 2008.
- 655 Rosenberry, D. O., Sheibley, R. W., Cox, S. E., Simonds, F. W. and Naftz, D. L.: Temporal
656 variability of exchange between groundwater and surface water based on high-frequency direct
657 measurements of seepage at the sediment-water interface, *Water Resour. Res.*, 49(5), 2975–2986,
658 doi:10.1002/wrcr.20198, 2013.
- 659 Rossi, P. M., Ala-aho, P., Doherty, J. and Kløve, B.: Impact of peatland drainage and restoration on
660 esker groundwater resources: modeling future scenarios for management, *Hydrogeol. J.*, 22, 1131–
661 1145, doi:10.1007/s10040-014-1127-z, 2014.
- 662 Rossi, P. M., Ala-aho, P., Ronkanen, a K. and Kløve, B.: Groundwater-surface water interaction
663 between an esker aquifer and a drained fen, *J. Hydrol.*, 432-433, 52–60,
664 doi:10.1016/j.jhydrol.2012.02.026, 2012.
- 665 Rozanski, K., Froehlich, K. and Mook, W. .: Surface water, in *Environmental isotopes in the*
666 *hydrological cycle. Principals and applications. Volume III. IHP-V. Technical Documents in*
667 *Hydrology*, vol. 111, edited by W. G. Mook, pp. 1–117, UNESCO/IAEA, Paris., 2001.
- 668 Schoch-Fischer, H., Rozanski, K., Jacob, H., Sonntag, C., Jouzel, J., Östlund, G. and Geyh, M. A.:
669 Hydrometeorological factors controlling the time variation of D, 18O and 3H in atmospheric water
670 vapour and precipitation in the westwind belt, in *Isotope Hydrology*, pp. 3–31, International Atomic
671 Energy Agency, Vienna., 1984.
- 672 Shaw, G. D., White, E. S. and Gammons, C. H.: Characterizing groundwater–lake interactions and
673 its impact on lake water quality, *J. Hydrol.*, 492, 69–78 [online] Available from:
674 <http://www.sciencedirect.com/science/article/pii/S0022169413003016> (Accessed 19 December
675 2013), 2013.
- 676 Showstack, R.: Discussion of challenges facing water management in the 21st century, *Eos, Trans.*
677 *Am. Geophys. Union*, 85(6), 58, doi:10.1029/2004EO060002, 2004.
- 678 Stets, E. G., Winter, T. C., Rosenberry, D. O. and Striegl, R. G.: Quantification of surface water and
679 groundwater flows to open- and closed-basin lakes in a headwaters watershed using a descriptive
680 oxygen stable isotope model, *Water Resour. Res.*, 46(3), 1–16, doi:10.1029/2009WR007793, 2010.
- 681 Stichler, W., Maloszewski, P., Bertleff, B. and Watzel, R.: Use of environmental isotopes to define
682 the capture zone of a drinking water supply situated near a dredge lake, *J. Hydrol.*, 362(3-4), 220–
683 233, doi:10.1016/j.jhydrol.2008.08.024, 2008.
- 684 Tikkanen, M.: The changing landforms of Finland, *Fennia*, 180(1-2), 21–30, 2002.
- 685 Turner, K. W., Wolfe, B. B. and Edwards, T. W. D.: Characterizing the role of hydrological
686 processes on lake water balances in the Old Crow Flats, Yukon Territory, Canada, using water
687 isotope tracers, *J. Hydrol.*, 386(1-4), 103–117, doi:10.1016/j.jhydrol.2010.03.012, 2010.

- 688 Winter, T. C. and Carr, M. R.: Hydrologic setting of wetlands in the Cottonwood lake area ,
689 Stutsman County, North Dakota. USGS Water-resources investigations report 80-99, Denver.,
690 1980.
- 691 Vogt, H. J.: Isotopentrennung bei der Verdunstung von Wasser, Staatsexamensarbeit, Institut für
692 Umweltphysik, Heidelberg., 1976.
- 693 Yehdeghe, B., Rozanski, K., Zojer, H. and Stichler, W.: Interaction of dredging lakes with the
694 adjacent groundwater field: and isotope study, J. Hydrol., 192, 247–270, 1997.
- 695 Yi, Y., Brock, B. E., Falcone, M. D., Wolfe, B. B. and Edwards, T. W. D.: A coupled isotope tracer
696 method to characterize input water to lakes, J. Hydrol., 350(1-2), 1–13,
697 doi:10.1016/j.jhydrol.2007.11.008, 2008.
- 698 Zimmerman, U.: Determination by stable isotopes of underground inflow and outflow and
699 evaporation of young artificial groundwater lakes, in Isotopes in lake studies, pp. 87–95,
700 International Atomic Energy Agency, Vienna., 1979.
- 701 Zuber, A.: On the environmental isotope method for determining the water balance components of
702 some lakes, J. Hydrol., 61(4), 409–427, 1983.
- 703
- 704
- 705
- 706
- 707
- 708
- 709

710 Table 1. Mean isotopic composition of selected lakes, streams and groundwater, sampled four times
 711 per year during the period 2010-2012.

	$\delta^2\text{H}$ (‰)	$\delta^{18}\text{O}$ (‰)	d-excess (‰)	Mean amplitude of $\delta^{18}\text{O}$ seasonal signal (‰)
Lakes:				
1. Ahveroinen 1	-72.4	-8.50	-4.42	1.2
2. Rokuanjärvi	-72.1	-8.75	-2.14	1.3
3. Jaakonjärvi	-64.1	-6.72	-10.34	0.8
4. Kolmonen 2	-66.7	-7.07	-10.14	0.9
5. Loukkojärvi	-63.0	-6.64	-9.88	0.9
6. Saarijärvi 2	-62.4	-6.81	-7.92	0.9
7. Saarinen	-72.3	-8.52	-4.14	3.3
8. Salminen	-71.4	-8.45	-3.80	0.5
9. Soppinen	-63.1	-6.84	-8.38	0.9
10. Tulijärvi	-85.6	-11.20	4.00	1.3
11. Vaulujärvi	-67.9	-7.68	-6.46	0.5
Streams:				
1. Heinäjoki	-93.0	-12.74	8.92	0.5
2. Hieto-oja	-88.9	-11.84	5.82	1.2
3. Kangasoja	-93.7	-12.90	9.50	0.7
4. Lianoja	-83.2	-10.67	2.16	2.2
5. Lohioja	-92.9	-12.93	10.54	0.8
6. Matokanava	-94.6	-13.06	9.88	0.9
7. Päiväkanava	-94.0	-13.01	10.08	0.9
8. Rokuanoja	-82.8	-10.95	4.80	3.1
9. Siirasoja	-94.6	-13.08	10.04	0.7
10. Soppisenoja	-89.9	-12.07	6.66	2.2
11. Valkiaisaja	-93.3	-12.80	9.10	1.0
Groundwater:				
1. MEA 106	-96.4	-13.32	10.16	0.6
2. MEA 206	-95.0	-13.12	9.96	0.8
3. MEA506	-93.5	-12.92	9.86	0.5
4. MEA 706	-93.3	-12.89	9.82	0.7
5. MEA 1106	-95.1	-13.05	9.30	0.8
6. MEA 1807	-93.3	-12.92	10.06	1.0
7. MEA 1907	-83.2	-10.65	2.00	1.0
8. MEA 2010	-97.3	-13.42	10.06	0.5
9. ROK 1	-95.5	-13.22	10.26	0.9
10. Siirasoja 1 esker	-94.5	-13.06	9.98	0.8
11. Siirasoja 1 slope	-94.3	-13.08	10.34	1.0
12. Siirasoja 1 sand	-97.0	-13.36	9.88	0.5
13. Siirasoja 1 peat	-93.8	-12.98	10.04	1.2

713 Table 2. The results of isotope mass balance calculations for 67 lakes of Rokua esker sampled during the July-August 2013 field survey.

Lake No.	Lake name	Volume (10 ³ m ³)	Surface area (ha)	Mean depth (m)	<i>E</i> ^(a) (mm)	δ ¹⁸ O (‰)	δ ² H (‰)	<i>I</i> _{GW} (m ³ /day)		<i>I</i> _{TOT} / <i>E</i>		MTT (month)		<i>G</i> index (%)	
								¹⁸ O	² H	¹⁸ O	² H	¹⁸ O	² H	¹⁸ O	² H
1	Heinälampi ^(b)	1764	0.22	0.8	286	-10.97	-84.4	71.5	67.3	14.2	13.3	0.6	0.6	72.4	73.0
2	Holma ^(b)	23778	1.89	1.3	257	-11.12	-84.8	569.3	520.7	15.8	14.2	0.9	1.0	68.4	69.5
3	Koivujärvi 1 ^(b)	39237	2.3	1.7	254	-11.38	-85.7	823.9	681.4	19.0	16.2	1.1	1.2	68.2	66.3
4	Koivujärvi 2 ^(b)	76884	2.93	2.6	251	-11.61	-87.3	1555.1	1393.4	20.6	18.5	1.5	1.7	94.1	93.9
5	Pitkäjärvi 1	36103	1.22	3	262	-6.50	-61.5	61.8	51.7	2.6	2.3	13.3	15.0	69.8	66.0
6	Nurkkajärvi	269134	3.93	6.8	247	-8.76	-73.1	407.7	362.8	4.7	4.2	17.8	19.5	82.5	80.8
7	Luontolampi	19995	0.49	4.1	275	-7.29	-64.9	34.6	28.6	3.1	2.7	14.4	16.6	76.4	72.8
8	Ahveroinen 1	119000	3.32	3.6	249	-8.80	-71.9	351.3	282.7	4.7	3.9	9.1	10.9	82.8	79.5
9	Lianjärvi ^(b)	113678	15.13	0.8	231	-10.31	-80.5	2375.0	2044.1	10.0	8.9	1.0	1.1	62.3	60.3
10	Syväjärvi 1 ^(b)	398463	11.52	3.5	234	-11.17	-85.3	3288.8	3030.3	12.7	11.7	3.5	3.8	88.3	88.1
11	Soppinen	81630	6.04	1.4	242	-7.60	-65.7	396.6	310.2	3.3	2.8	5.0	6.0	74.9	70.0
12	Salminen	681860	25.31	2.7	225	-8.59	-70.7	2177.5	1724.8	4.4	3.7	8.1	9.8	79.7	75.6
13	Saarinen	981506	15.32	6.4	231	-8.22	-69.4	1186.0	974.2	4.0	3.4	21.0	24.4	77.9	74.3
14	Kivi-Ahveroinen	216018	5.57	3.9	243	-9.02	-74.4	623.6	556.9	5.1	4.6	9.4	10.4	83.6	82.0
15	Irvi-Ahveroinen	40867	1.07	3.8	264	-7.47	-65.6	76.2	62.1	3.3	2.8	13.4	15.6	76.5	72.6
16	Loukkojärvi	126450	2.85	4.4	251	-7.10	-65.6	166.8	153.3	2.9	2.8	18.0	19.1	72.7	71.0
17	Ylimmäinen	94313	8.93	1.1	237	-9.66	-77.6	1252.1	1130.9	6.3	5.8	2.1	2.3	86.5	85.2
18	Hietajärvi	223118	7.3	3.1	240	-7.06	-63.7	394.5	318.7	2.9	2.5	13.1	15.2	71.1	66.5
19	Saarijärvi 2	2467169	20.94	11.8	228	-6.72	-62.2	924.6	747.2	2.7	2.3	58.1	66.7	66.8	61.9
20	Syväjärvi 2 ^(b)	1863446	31.95	5.8	223	-10.63	-83.1	7668.9	7328.2	12.0	11.3	6.5	6.9	82.3	83.5
21	Pasko ^(b)	2005	0.82	0.2	268	-10.62	-83.3	189.6	185.8	10.8	10.5	0.3	0.3	73.8	74.4
22	Kuikkalampi	11776	0.61	1.9	271	-7.20	-66.6	41.5	39.7	3.0	2.9	7.0	7.2	75.5	74.7
23	Soppisenlampi	25645	0.59	4.4	272	-7.32	-67.1	41.4	39.4	3.1	3.0	15.4	16.0	76.3	75.4
24	Kirvesjärvi	654618	13.47	4.9	233	-11.45	-87.6	5195.9	5601.3	18.5	19.5	3.4	3.2	82.4	84.1
25	Tulijärvi ^(b)	589617	24.81	2.4	226	-10.40	-81.7	4650.7	4428.9	10.9	10.3	2.9	3.1	69.9	70.8
26	Jaakonjärvi 2	5497	0.46	1.2	275	-7.39	-65.3	34.1	27.9	3.2	2.7	4.1	4.7	77.1	73.3
27	Jaakonjärvi 3	13594	0.66	2.1	271	-7.60	-66.4	50.7	41.8	3.4	2.9	6.8	7.9	77.9	74.3
28	Maitolampi 2	44812	2.04	2.2	256	-7.52	-65.9	142.0	115.8	3.3	2.8	7.8	9.1	76.1	72.2

29	Kotalampi	25980	2.6	1	253	-11.23	-86.3	860.9	877.7	12.9	13.1	0.9	0.9	93.8	93.9
30	Rokuanjärvi 1	4364781	164.59	2.7	205	-9.11	-71.8	15206.8	10695.0	5.1	3.9	7.6	9.9	80.8	74.7
31	Tervatienlampi	21970	0.63	3.5	271	-7.92	-69.3	54.3	49.5	3.7	3.4	10.5	11.3	79.8	78.2
32	Valkiaislampi	32073	0.7	4.6	270	-8.81	-72.5	82.5	69.6	4.8	4.1	10.7	12.3	84.3	81.9
33	Ankkalampi	103700	3.86	2.7	248	-8.57	-71.9	373.5	326.9	4.4	4.0	7.4	8.2	81.5	79.4
34	Saarilampi 1	12044	0.45	2.7	276	-10.51	-80.8	110.5	91.2	8.9	7.5	3.3	3.9	91.8	90.2
35	Kiiskeroinen	6517	0.63	1	271	-12.14	-90.2	482.7	447.8	26.6	24.8	0.4	0.5	97.2	97.0
36	Jaakonjärvi 1	93614	3.53	2.7	249	-6.82	-63.5	184.2	159.3	2.7	2.5	11.7	12.9	70.4	67.3
37	Vaulujärvi	432813	8.97	4.8	237	-7.84	-68.6	628.9	553.8	3.6	3.2	17.1	18.8	76.2	73.8
38	Levä-Soppinen	34000	2.31	1.5	254	-12.27	-91.4	1922.5	2060.2	31.0	33.1	0.6	0.5	97.4	97.6
39	Anttilanjärvi	60230	1.06	5.7	264	-7.40	-66.4	73.8	64.9	3.2	2.9	20.3	22.3	76.1	73.7
40	Hautajärvi 1	189222	2.56	7.4	253	-7.71	-68.0	187.0	165.8	3.5	3.2	25.4	27.8	76.9	74.7
41	Lepikonjärvi	191118	2.98	6.4	251	-7.77	-68.3	220.2	195.8	3.5	3.2	21.8	23.9	77.1	75.0
42	Kolmonen 1	35700	0.68	5.3	270	-7.09	-65.2	43.9	39.5	3.0	2.7	19.8	21.4	74.7	72.7
43	Kolmonen 2	21890	0.56	3.9	273	-7.25	-65.8	38.5	34.1	3.1	2.8	14.1	15.4	75.9	73.6
44	Kolmonen 3	21630	0.54	4	273	-7.26	-66.1	37.4	33.9	3.1	2.9	14.3	15.4	76.0	74.2
45	Hätäjärvi	35217	1.73	2	258	-6.50	-61.8	85.4	72.8	2.5	2.3	9.3	10.4	69.2	65.7
46	Kissalampi	800	0.36	0.2	279	-5.60	-57.1	14.5	11.8	2.1	1.8	1.2	1.3	64.9	60.2
47	Valkiajärvi	582662	8.36	7	238	-8.49	-71.2	747.9	637.5	4.3	3.8	20.4	23.1	80.3	77.6
48	Hautajärvi 2	445413	14.6	3.1	232	-7.43	-64.5	857.1	646.0	3.2	2.6	12.3	15.0	72.8	66.8
49	Keskimmäinen ^(b)	428515	13.07	3.3	233	-10.76	-82.8	3117.4	2686.0	10.9	9.6	3.9	4.4	86.4	84.8
50	Siirasjärvi 2	23126	0.56	4.1	273	-12.66	-93.5	977.5 ^(d)	1315.5 ^(d)	59.7 ^(d)	80.1 ^(d)	0.8 ^(d)	0.6 ^(d)	98.8 ^(d)	99.1 ^(d)
51	Siirasjärvi 1	9701	0.34	2.9	280	-10.43	-80.4	81.5	66.8	8.6	7.2	3.6	4.3	91.6	90.0
52	Telkkälampi	7284	0.25	2.9	284	-7.30	-66.3	18.7	16.9	3.1	2.9	9.8	10.6	77.2	75.4
53	Maitolampi 1	48892	1.56	3.1	259	-6.36	-61.2	73.8	63.3	2.5	2.2	14.8	16.4	68.4	64.9
54	Taka-Salminen ^(b)	364757	7.31	5	240	-9.63	-76.2	772.6	609.0	7.8	6.4	8.0	9.7	52.3	49.6
55	Etu-Salminen ^(b)	196453	5.83	3.4	243	-8.05	-68.5	311.7	259.3	5.1	4.3	8.2	9.6	39.9	38.9
56	Pikku-Salminen	39856	1.32	3	261	-7.61	-65.8	97.4	76.9	3.4	2.8	10.3	12.3	77.1	72.7
57	Kylmäjärvi	394443	7.89	5	239	-8.47	-70.3	703.3	564.6	4.3	3.6	14.7	17.4	80.2	76.5
58	Kourujärvi 1	68023	1.83	3.7	257	-8.55	-71.7	183.8	159.9	4.4	3.9	9.9	11.1	82.1	80.0
59	Kourujärvi 2	31136	1.91	1.6	256	-7.64	-67.3	139.5	120.6	3.4	3.1	5.6	6.2	76.9	74.2
60	Huttunen	54588	1.49	3.7	260	-7.50	-66.9	105.6	92.7	3.3	3.0	12.9	14.2	76.3	73.9

61	Saarijärvi 1	13590	1.36	1	261	-6.49	-61.4	68.1	56.8	2.5	2.2	4.5	5.1	69.5	65.5
62	Pitkäljärvi 2	451093	7.93	5.7	239	-8.05	-68.7	607.3	505.3	3.8	3.3	18.8	21.6	77.7	74.4
63	Pyöräinen ^(b)	76077	3.76	2	248	-7.91	-67.9	270.8	224.5	4.8	4.1	5.1	6.0	56.0	54.6
64	Likainen ^(b)	33763	8.28	0.4	238	-10.94	-83.4	2110.9	1732.2	13.2	11.2	0.4	0.5	74.8	71.9
65	Nimisjärvi ^{(b), (c)}	1840396	167.53	1.1	205	-8.66	-69.7	15759.0	11551.0	5.2	4.1	3.1	3.9	81.1	75.8
66	Ahveroinen 2 ^(b)	670515	16.3	4.1	230	-7.96	-67.8	1077.3	854.5	4.3	3.6	12.4	14.7	61.2	57.6
67	Tervalampi	29707	0.79	3.7	268	-7.99	-68.7	69.3	58.8	3.7	3.3	11.2	12.7	79.9	77.1

714 (a) - Calculated for the period June 1 - August 31, 2013.

715 (b) - Lakes with identified surface inflow from an upstream lake.

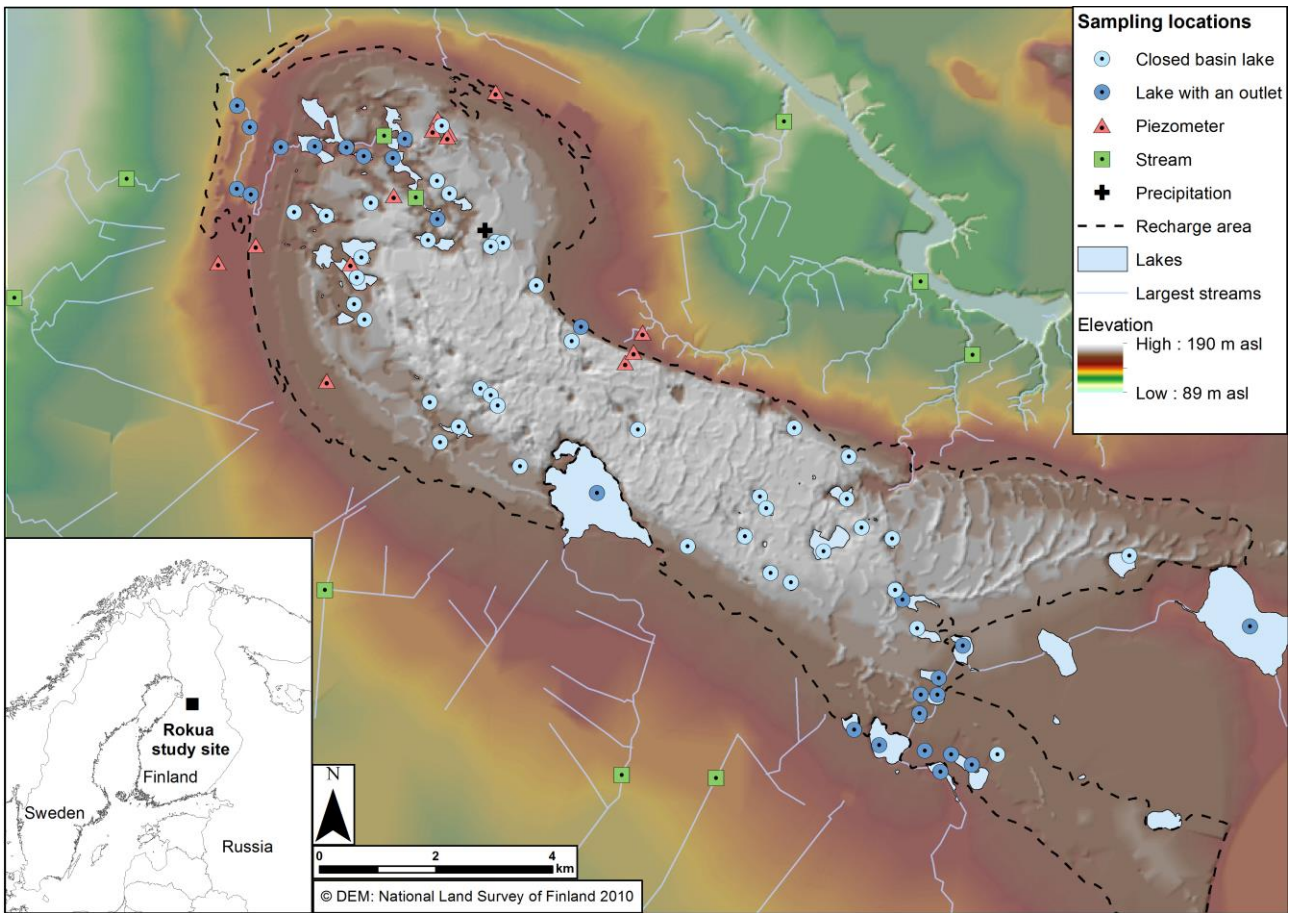
716 (c) - Since the upstream lake for lake Nimisjärvi was not sampled, the mean isotopic composition of total inflows to lakes with identified surface water
717 inflows was used for isotope mass balance calculations of this particular lake.

718 (d) - As the isotopic composition of a lake becomes comparable with the isotopic composition of the total inflow, the isotope mass balance calculations
719 become very uncertain. Therefore, for lake Siirasjärvi 2 ($\Delta\delta^{18}\text{O} = 0.45\text{‰}$ and $\Delta\delta^2\text{H} = 1.6\text{‰}$) the values of I_{TOT}/E , MTT and G index reported in the
720 table have only an indicative character.

721 Table 3. Sensitivity of selected elements of ^{18}O -based water balance of the studied lakes to changes
 722 of the parameters involved.
 723

Parameter	Parameter change	Mean change of the selected elements of water balance (%) ^(a) :		
		I_{TOT}/E	MTT	G index
1. Lake water temperature ($T_w = 19.1$ °C)	+0.87 °C	-0.9	-11.7	+2.9
	-0.87 °C	+0.7	+15.0	-3.6
2. Normalized relative humidity ($h_N = 60.7$ %)	+2.0 %	-1.5	+7.0	-1.9
	-2.0 %	+1.3	-6.2	+1.6
3. Isotopic composition of atmospheric water vapour ($\delta^{18}\text{O}_A = -20.4$ ‰)	+1.0 ‰	+7.6	-7.1	+1.7
	-1.0 ‰	-7.6	+8.2	-2.0
4. Isotopic composition of lake water ($\delta^{18}\text{O}_{\text{LS}}$)	+0.5 ‰	-15.8	+19.6	-3.3
5. Isotopic composition of the total inflow ($\delta^{18}\text{O}_{\text{IT}}$)	+0.5 ‰	+20.2	-14.8	+4.4

724 (a) The (+) and (-) signs signify an increase or reduction, respectively, of the derived quantity by the reported
 725 percentage.
 726



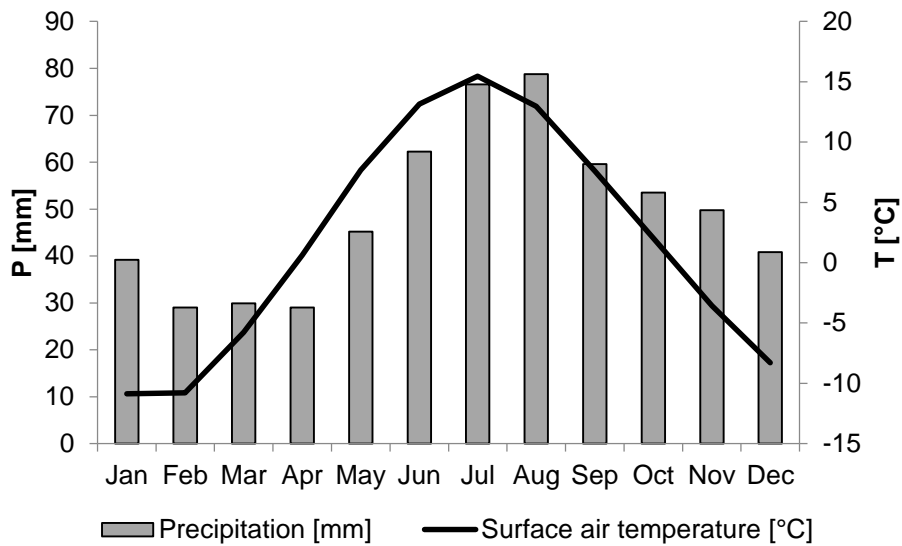
728

729 Figure 1. The study site of Rokua esker aquifer area. Digital elevation model by the National Land
730 Survey of Finland (2010).

731

732

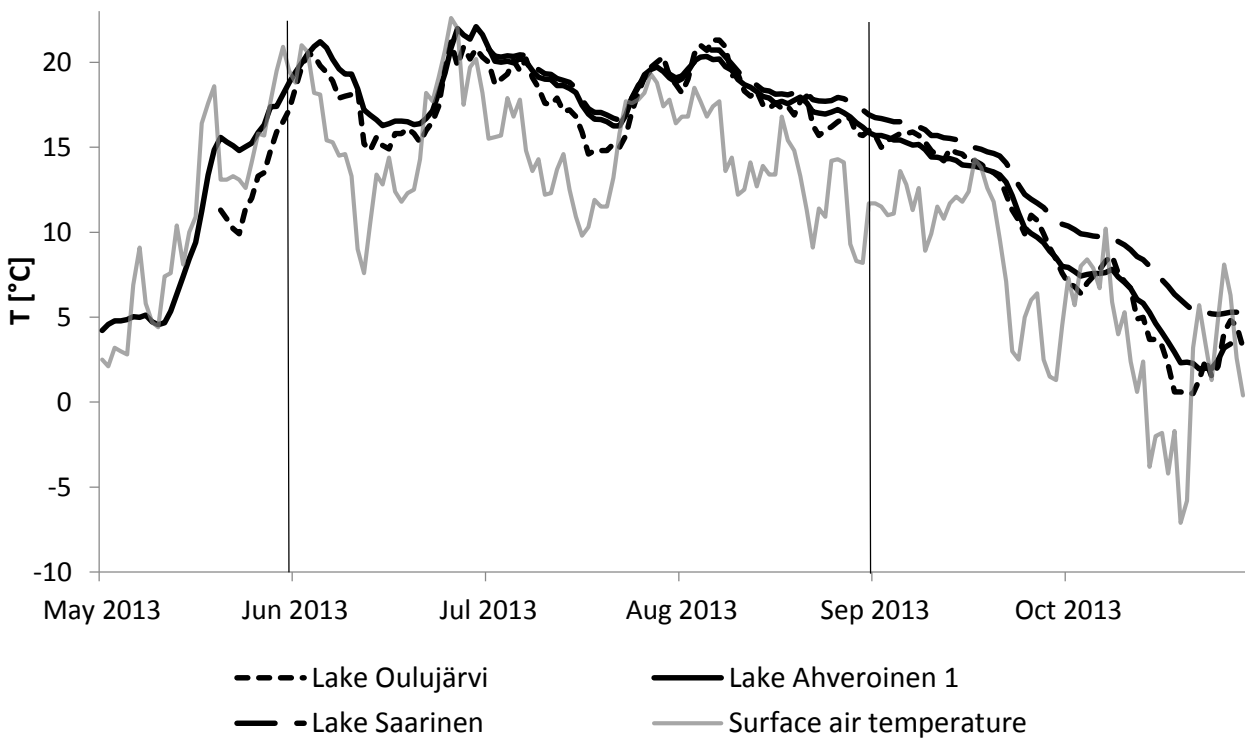
733



734

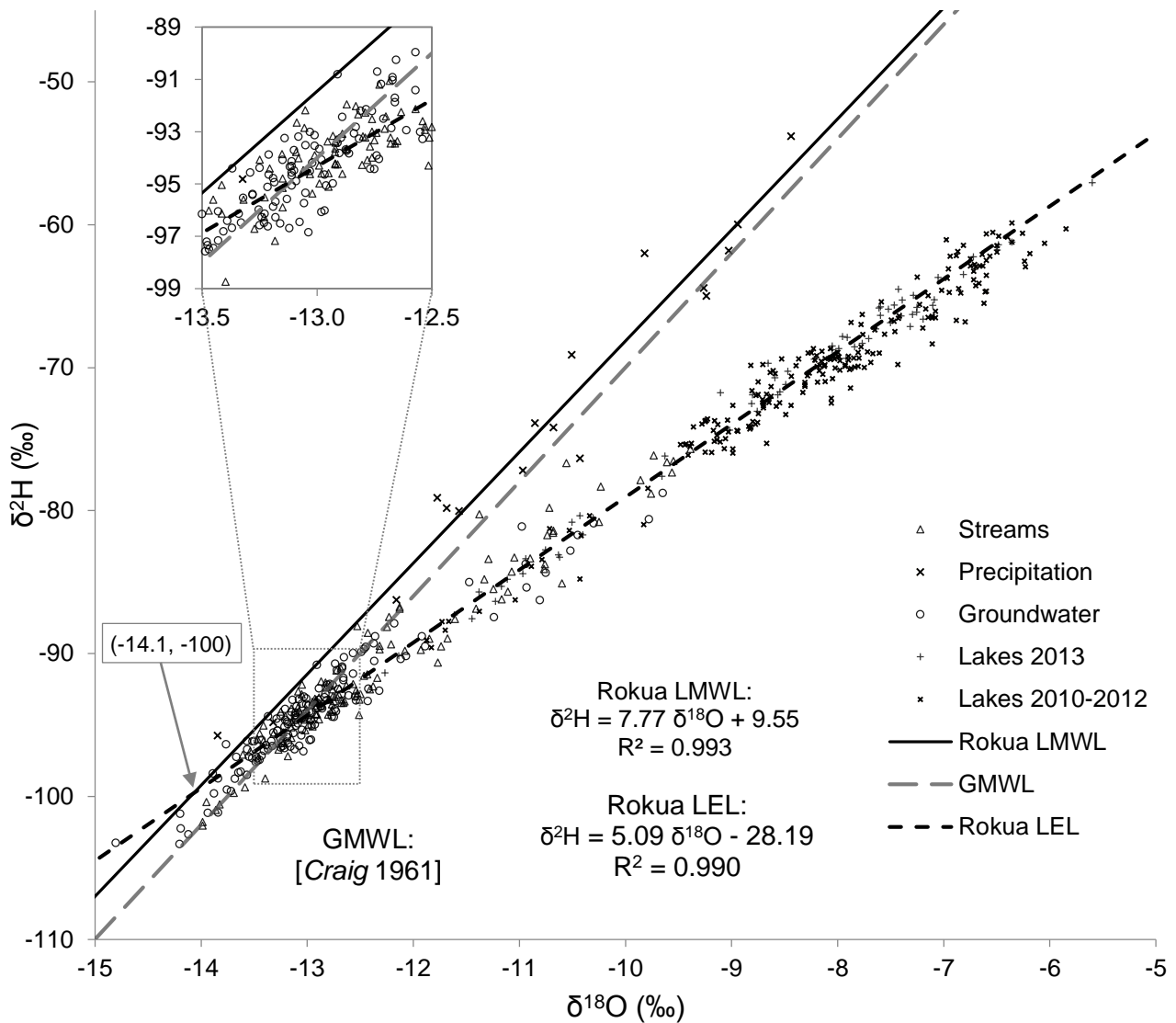
735 Figure 2. The long-term (1959-2013) monthly mean values of surface air temperature and the amount
 736 of precipitation recorded at the station located 10 km south-west of the study site (Finnish
 737 Meteorological Institute, 2014).

738

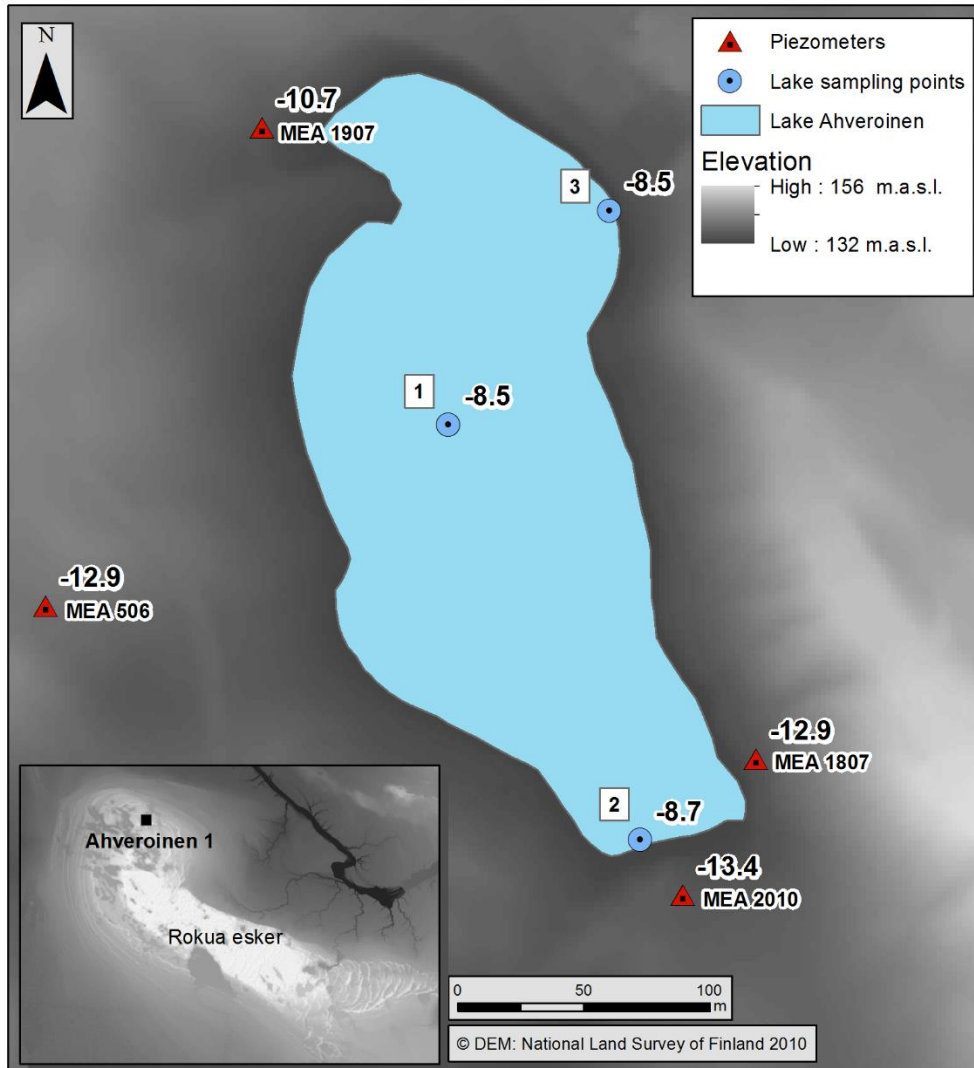


739

740 Figure 3. Daily mean surface water temperatures of lakes Oulujärvi (92,800 ha) (Finnish
 741 Environmental Institute, 2013), Ahveroinen 1 (3.3 ha) and Saarinen (15.3 ha) during the summer of
 742 2013, compared with the surface air temperature data for the same period. Lake Oulujärvi is located
 743 in the east, next to the study site, 1 km from the easternmost lake studied. Vertical lines mark the
 744 period used in the calculations of evaporation and isotope mass balance.

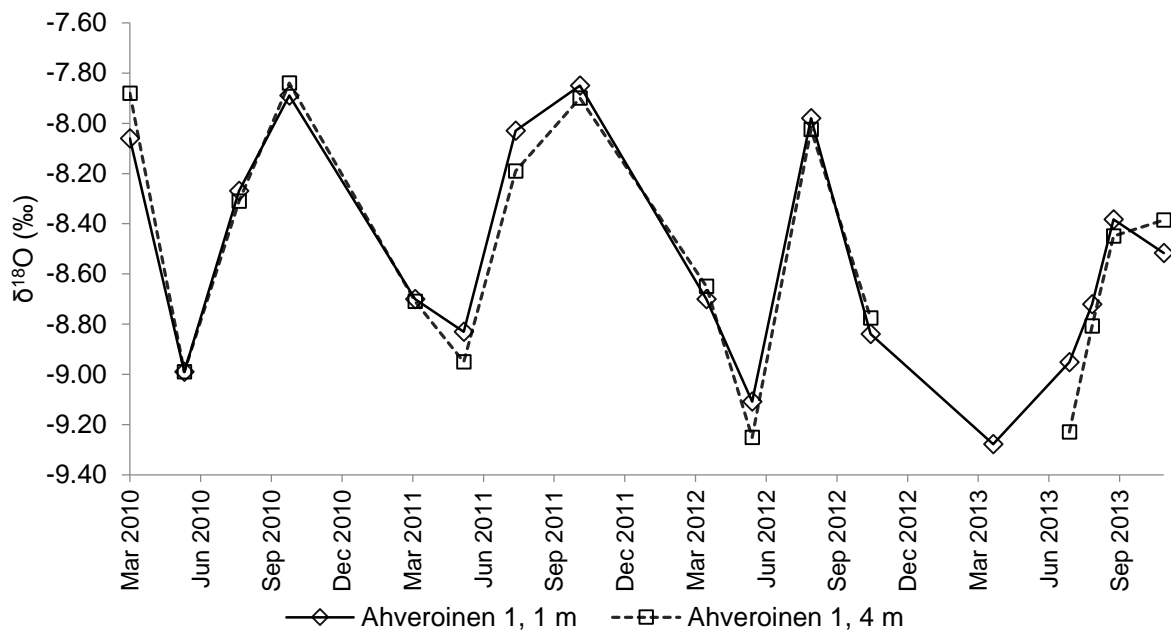


745
 746 Figure 4. $\delta^2\text{H}$ - $\delta^{18}\text{O}$ relationship for different appearances of surface water (lakes, streams) and
 747 groundwater in the study area, investigated within the scope of this study. The Rokua evaporation
 748 line (local evaporation line - LEL) was defined as the best fit line of the data points representing lakes
 749 sampled during the July-August 2013 campaign.
 750



751
752
753
754

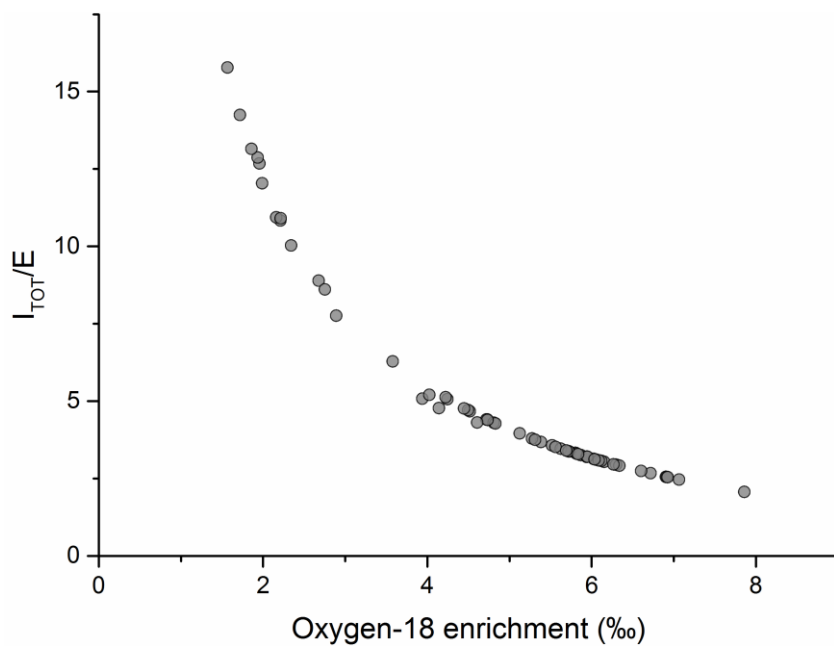
Figure 5. Mean $\delta^{18}\text{O}$ values (‰) of lake Ahveroinen and adjacent groundwater. The mean $\delta^{18}\text{O}$ value for site 1 is 8.5 ‰ at both sampled depths (1 m and 4 m).



755

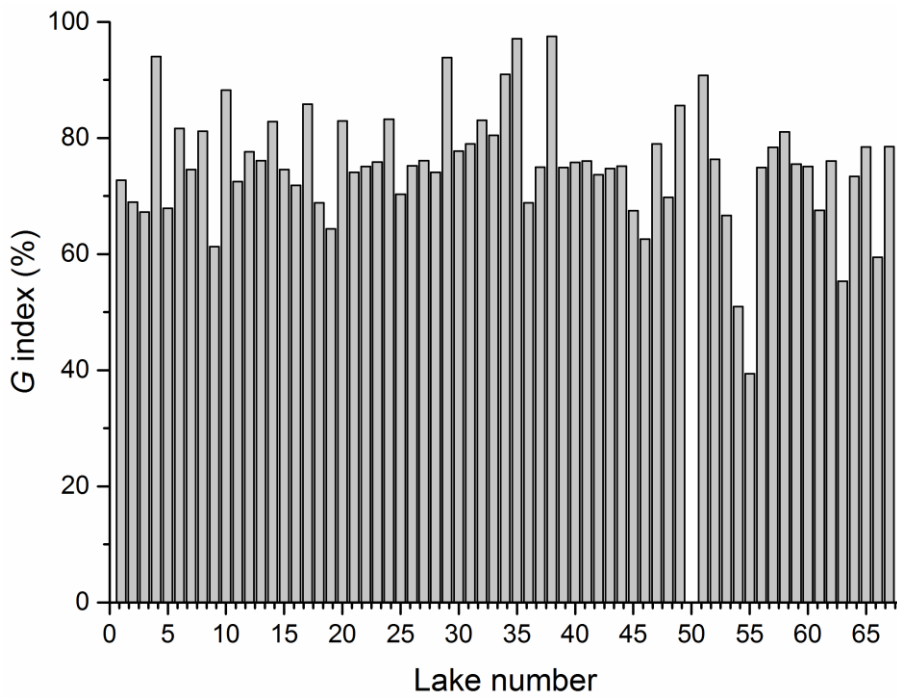
756 Figure 6. Seasonal variations of $\delta^{18}\text{O}$ in lake Ahveroinen 1, observed at 1 and 4-meter depths.
 757 Maximum depth of the lake is 4.8 m.

758



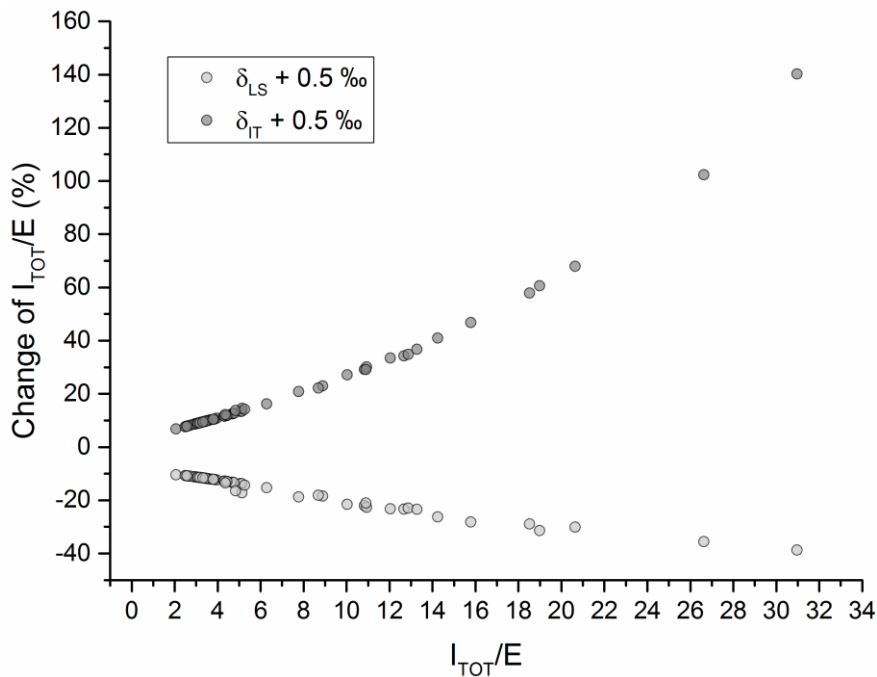
759

760 Figure 7. The ratio of total inflow to evaporation (I_{TOT}/E) as a function of the measured ^{18}O isotope
 761 enrichment ($\Delta\delta^{18}\text{O}$) for Rokua lakes surveyed during the July-August 2013 sampling campaign.



762

763 Figure 8. The G index quantifying the groundwater dependency of lakes in the Rokua study area. The
 764 index is defined as the percentage contribution of groundwater inflow to the total inflow of water to
 765 the given lake. Shown are the mean G values obtained from independent isotope mass balance
 766 calculations based on ^2H and ^{18}O data.



767

768 Figure 9. Changes of the total inflow-to-evaporation ratio (in %) based on ^{18}O isotope mass balance
 769 as a function of I_{TOT}/E value, in response to parameter change, calculated for the studied lakes on the
 770 Rokua esker. Two cases are considered: (a) an increase of the measured $\delta^{18}\text{O}$ of lake water by 0.5 ‰,
 771 and (b) an increase of $\delta^{18}\text{O}$ of the total inflow to the given lake by 0.5 ‰. See text for details.
 772